SSC-275

THE EFFECT OF STRAIN RATE ON THE TOUGHNESS OF SHIP STEELS

This document has been approved
for public release and sale; its
distribution is unlimited.

SHIP STRUCTURE COMMITTEE
1978

Member Agencies:
United States Coast Guard
Naval Sea Systems Command
Military Sealift Command
Maritime Administration
United States Geological Survey
American Bureau of Shipping

Ship Structure Committee

An Interagency Advisory Committee
Dedicated to Improving the Structure of Ships

Address Correspondence to:
Secretary, Ship Structure Committee
U.S. Coast Guard Headquarters,(G-M/82)
Washington, D.C. 20590

SR-1231
JULY 1978

Material requirements and design procedures to avoid catastrophic fractures of ship hull structures continue to be of great concern to designers. The Ship Structure Committee has undertaken a program to define and formulate fracture toughness criteria for steels up to 100,000 psi yield strengths and their associated weldments.

SSC-244 contains a critical review and assessment of current knowledge of ship steel behavior and a proposed fracture criteria. SSC-244 provides small-scale experimental data from essentially static loading and one dynamic impact loading. SSC-276 offers additional larger scaled data.

The present report, SSC-275, develops data on a variety of ship steels at various loading rates and temperatures to assist in setting the fracture criteria limits within the service loading spectrum.

W. M. Benkert
W. M. Benkert
Rear Admiral, U.S. Coast Guard
Chairman, Ship Structure Committee

FINAL REPORT

on

Project SR-1231

"Fracture Criteria Based on Loading Rates"

THE EFFECT OF STRAIN RATE ON THE TOUGHNESS OF SHIP STEELS

by

P. H. Francis
T. S. Cook
A. Nagy

Southwest Research Institute

under

Department of the Navy
Naval Sea Systems Command
Contract No. N00024-75-C-4284

This document has been approved for public release and sale; its distribution is unlimited.

U. S. Coast Guard Headquarters
Washington, D.C.
1978

ABSTRACT

Yield strength and fracture toughness, as measured by the dynamic tear test, were determined as a function of load rate and temperature for several ship primary structure steels in strength ranges up to 100 ksi. The materials used were ABS-B, DS, AH-32, EH-32, CS, A517-D, A678-C, and A537-B, in one or two heats each. The effect of notch geometry, i.e., fatigue precracked vis-a-vis pressed notch, was investigated in some of the tests.

By fully instrumenting some of the tests, the energy to maximum load as well as the total energy to failure was determined. Based on these energies, the resistance of the materials to crack initiation and to propagation could be examined. The results indicate potentially different fracture behavior between the high and low strength alloys. This in turn has implications in terms of the Ship Structure Committee Report SSC-244 proposed fracture criterion for qualifying toughness and crack arrest properties of ship steels and weldments.

TABLE OF CONTENTS

LIST OF ILLUSTRATIONS

LIST OF ILLUSTRATIONS (Cont'd)

LIST OF TABLES

LIST OF TABLES

LIST OF SYMBOLS

k	Boltzmann constant
K	stress intensity factor
K_1	mode 1 stress intensity factor
$\dot{K}$	time rate of K
$\dot{K}_1$	time rate of K_1
K_C, J_C	measures of notch toughness
K_{Cd}	dynamic notch toughness
K_{1C}	mode 1 fracture toughness
K_{1d}	dynamic mode 1 fracture toughness
P	load
r_p	characteristic dimension of plastic zone
T	absolute temperature
T_s	reference (room) temperature
U	activation energy
V	activation volume
W_f	energy to fracture
W_m	energy to maximum load
x	displacement
α_1, α_2	constants
$\dot{\varepsilon}$	strain rate
$\dot{\varepsilon}_o$	viscosity coefficient
$\dot{\varepsilon}_s$	"static" strain rate
σ_i	athermal stress field
σ_o	σ_i + U/V

σ_y, σ_{ys}	"static" yield strength
σ_{yd}	"dynamic" yield strength
σ_y'	dynamic overstress

SHIP STRUCTURE COMMITTEE

The SHIP STRUCTURE COMMITTEE is constituted to prosecute a research program to improve the hull structures of ships and other marine structures by an extension of knowledge pertaining to design, materials and methods of construction.

RADM W. M. Benkert (Chairman)
Chief, Office of Merchant Marine Safety
U. S. Coast Guard Headquarters

Mr. P. M. Palermo
Assistant for Structures
Naval Ship Engineering Center
Naval Sea Systems Command

Mr. W. N. Hannan
Vice President
American Bureau of Shipping

Mr. M. Pitkin
Assistant Administrator for Commercial Development
Maritime Administration

Mr. R. B. Krahl
Chief, Branch of Marine Oil and Gas Operations
U. S. Geological Survey

Mr. C. J. Whitestone
Chief Engineer
Military Sealift Command

LCDR T. H. Robinson, U. S. Coast Guard (Secretary)

SHIP STRUCTURE SUBCOMMITTEE

The SHIP STRUCTURE SUBCOMMITTEE acts for the Ship Structure Committee on technical matters by providing technical coordination for the determination of goals and objectives of the program, and by evaluating and interpreting the results in terms of structural design, construction and operation.

U. S. COAST GUARD

Lcdr J. C. Card
Lcdr S. H. Davis
Capt C. B. Glass
Dr. W. C. Dietz

NAVAL SEA SYSTEMS COMMAND

Mr. R. Chiu
Mr. R. Johnson
Mr. G. Sorkin
Mr. J. B. O'Brien (Contracts Admin.)

MARITIME ADMINISTRATION

Mr. F. J. Dashnaw
Mr. N. O. Hammer
Mr. F. Seibold
Mr. M. Touma

NATIONAL ACADEMY OF SCIENCES SHIP RESEARCH COMMITTEE

Mr. O. H. Oakley - Liaison
Mr. R. W. Rumke - Liaison

SOCIETY OF NAVAL ARCHITECTS & MARINE ENGINEERS

Mr. A. B. Stavovy - Liaison

WELDING RESEARCH COUNCIL

Mr. K. H. Koopman - Liaison

MILITARY SEALIFT COMMAND

Mr. T. W. Chapman
Mr. A. B. Stavovy
Mr. D. Stein
Mr. J. Torresen

AMERICAN BUREAU OF SHIPPING

Dr. H. Y. Jan
Mr. D. Liu
Mr. I. L. Stern
Mr. S. G. Stiansen (Chairman)

U. S. GEOLOGICAL SURVEY

Mr. R. Giangerelli
Mr. J. Gregory

INTERNATIONAL SHIP STRUCTURES CONGRESS

Prof. J. H. Evans - Liaison

AMERICAN IRON & STEEL INSTITUTE

Mr. R. H. Sterne - Liaison

STATE UNIV. OF NEW YORK MARITIME COLLEGE

Dr. W. R. Porter - Liaison

U. S. COAST GUARD ACADEMY

Capt W. C. Nolan - Liaison

U. S. NAVAL ACADEMY

Dr. R. Battacharyya - Liaison

U. S. MERCHANT MARINE ACADEMY
Dr. Chin-Bea Kim - Liaison

I. INTRODUCTION

A. Research Objectives

In its quest to improve the safety and reliability of welded ship hulls, the Ship Structure Committee has initiated a series of projects in recent years aimed at developing suitable criteria for qualifying structural steels and weldments. In one of the earlier reports on this series of projects, SSC-244, Rolfe, et. al.[1], proposed a tentative criterion for ensuring adequate fracture resistance of a wide range of ship steels and weldments for primary and secondary structural applications. In a subsequent report, SSC-248, Hawthorne and Loss at the NRL[2] developed a limited data base on 1-inch thick ship steels and weldments for the purpose of evaluating, at least in a limited way, the SSC-244 criterion.

The present work was undertaken to expand upon the NRL work cited above, in order that a more comprehensive assessment of the proposed criteria would be possible. This was done by conducting a mechanical testing program on various heats of seven grades of ship steel, ranging from as-rolled, through normalized, and up to high strength, Q & T alloys. In particular, one or two heats each of ABS-B, DS, AH, EH, CS, ASTM A517-D, A678-C, and A537-B were selected for fabrication of specimens. The experimental work was aimed at determining the effect of load rate and temperature on the yield strength and fracture behavior of these various classes of ship steels. Accordingly, tensile tests and dynamic tear (DT) tests were conducted at various loading rates and temperatures.

The test program was designed to probe several material and specimen parameters. This report presents the final results in detail. It then compares the results with the proposed SSC-244 requirements [1] for the materials involved and with the SSC-248 preliminary data.[2] Finally, an attempt was made to evaluate the adequacy of the criterion in light of the present findings.

The present project is a companion to another project[3] also being conducted at SwRI entitled "Fracture Behavior Characterization Of Ship Steels And Weldments." In that project, which was conducted in parallel with the present one, the emphasis was on fracture behavior of manual and submerged arc automatic welded specimens, as measured primarily by Charpy, DT, explosion crack starter, and explosion tear tests.

B. Review Of Load Rate Effects On Mechanical Performance

Ships operate in dynamic environments; ship structure is thus subject to dynamic loads from a variety of sources. Most important from a primary structure standpoint are those loads associated with wave crest/trough effects as they interact with the ship hull. These effects create time-dependent cyclic longitudinal and torsional bending moments on the structure as well as transient slamming pressures and springing response as the bow pitches in and out of the sea. Dynamic loading effects are caused also by moving cargos (as in LNG tankers), unbalanced shipboard machinery, thermal, aircraft landing, weapons, and docking loads, and these sources can become important in particular circumstances. Dynamic load effects are important to address in ship structural design, not only because they serve to establish the peak service load conditions, but also because the performance of the structural material can be sensitive to load rate effects.

There are two ways in which ship structural steel will exhibit load rate effects. The first of these is in the strength properties. Nearly all steels show an increase in yield strength with load rate. The degree of dependency of strength on load rate depends upon the strength level itself; ordinary-strength low carbon steels are the most sensitive to load rate effects, while quenched and tempered and HSLA steels, on the other hand, are much less strongly affected. Weldments, the region of prime structural design concern, also are sensitive to load (strain) rate. In general, the dynamic yield strength, σ_{yd}, of a particular material depends both upon temperature and strain rate according to a relationship of the form $\sigma_{yd} = \sigma_y(T, \dot{\varepsilon}) \approx \frac{\ell n\, \dot{\varepsilon}}{T}$, where T is the absolute temperature. This expression reveals that yield strength is inversely proportional to absolute temperature and is logarithmically related to the strain rate $\dot{\varepsilon}$.

Very little has been done thus far to establish the temperature and strain-rate dependence of the yield strength for ship steels and weldments. In developing their fracture criterion for ship steels, Rolfe et. al [1] assumed that "dynamic" yield strength was 20 ksi greater than "static" yield strength, for all relevant steels and load rates. One of the primary objectives of the present research program is to develop a data base on a class of ship steels which will enable a careful assessment of this assumption.

In addition to the effect of load rate on strength, load rate also affects fracture performance. It is usual to view fracture initiation and fast fracture as separate physical processes, although this distinction is often fuzzy. Fracture initiation is concerned with the material's ability to resist initial flaw formation, as contrasted with the conditions needed to drive an established crack toward global fracture. In many cases it is difficult to draw a clear distinction when conducting and analyzing a fracture test. The key parameter in the understanding of fracture behavior is the fracture toughness, the maximum value the crack tip stress intensity factor K_I can assume before stable crack growth or fast fracture develops. In discussing rate effects on fracture toughness it is convenient to express the dynamic fracture toughness as K_{1d}.

It should be noted that the dynamic fracture toughness, K_{1d}, is used differently by different authors, so some care must be exercised to ensure consistency. As commonly used, dynamic fracture toughness refers to (i), the toughness of a material measured according to ASTM static toughness requirements except for rate of application of load, or (ii), the toughness of a material ahead of a rapidly propagating crack. The two terms are often used interchangably on the basis of an argument by Krafft[4]. He reasoned that for a volume element within the fracture process zone near a crack, it makes no difference whether the deformation arises from rapid loading at a fixed crack length or the rapid approach of a crack with the load fixed; the local effect of time of deformation should be the same. To substantiate this, Eftis and Krafft[5] sought to compare the initiation and rapid propagation of a crack in the mild steel plate. They suggested that at a constant temperature, fracture toughness will decrease with increasing strain rate to some minimum level. They further postulated that the high strain rates where the minimum toughness occurred could be obtained from either rising load crack initiation tests or from data of a running crack. Although the behavior was not firmly established for all materials, the tests did indicate that the use of very high loading rates for crack initiation tests should lead to minimum K_{1d} values necessary for conservative design practices.

Available data[4] suggest that K_{1d} varies inversely as the logarithm of dK/dt for steels of the type considered here. The curves are log-log linear, indicating that dynamic fracture toughness is inversely proportional to the logarithm of loading rate $\dot{\varepsilon}$. Also, K_{1d} increases with temperature, in contrast to yield strength. These observations lead to the conclusion that dynamic fracture toughness must be related to (absolute) temperature T and load rate $\dot{K}$ ($= dK/dt$) by an expression of the form $K_{1d} \approx \alpha_1 T + \alpha_2/\dot{K}$, where α_1 and α_2 are constants. Now, according to the fracture toughness criterion proposed by Rolfe, et. al.[1], the fracture toughness required of ship steel can be expressed as the ratio $K_{1d}/\sigma_{yd} \geq 0.9 \sqrt{\text{in.}}$ at minimum service temperature (32°F). This requirement is to ensure that the steel has adequate ductility or elasto-plastic fracture response at the minimum operating temperature. On expressing the ratio K_{1d}/σ_{yd} in terms of the relations stated earlier, one concludes that the criterion regarding K_{1d}/σ_y is very sensitive to T, depends less strongly upon $\dot{K}$, and only weakly upon $\dot{\varepsilon}$. In other words, insofar as load rates ($\dot{K}$ and $\dot{\varepsilon}$) are concerned, fracture toughness is much more sensitive to the time rate of change of the crack tip stress intensity factor ($\dot{K}_1$) than to overall material strain rates ($\dot{\varepsilon}$).

Following the early efforts at NRL, much of the subsequent work concerned with load rate effects on toughness was aimed more at development of testing methods and small specimens than at rate effects per se. (To emphasize this, many investigators dropped the dynamic subscript on toughness and reverted to the static designation, K_{IC}). Shoemaker[6] presented dynamic data on a structural steel which showed no effect of strain rate on K_{IC} over a temperature range of -286°F to -70°F. There was an effect noted on the temperature at which transition from K_{IC} to K_C behavior took place, however.

In a similar set of tests, Shoemaker and Rolfe[7, 8] contended that Krafft's claim of a minimum loading rate [4] had not been substantiated. They were able to find a correlation between the rate parameter

$$R = T \ln A/\dot{\varepsilon}$$

and the toughness, with the degree of correlation varying for different materials. For ABS-C steel, a toughness value of 50 ksi $\sqrt{\text{in.}}$ was obtained under static conditions at -200°F whereas the same value at -10°F was obtained for dynamic loading; these values fit the rate parameter correlation. A further result was that for this same steel, an estimate of the dynamic toughness, K_{Id} value at the NDT from the dynamic yield stress was in good agreement with the measured toughness. This result indicated that Krafft was correct in this prediction of a minimum toughness at high loading rates. However, the result did not hold for two higher strength steels.

Dynamic fracture initiation properties are generally carried out using instrumented Charpy, drop-weight, or dynamic tear impact testing methods. The instrumented Charpy test involves the use of a precracked Charpy specimen together with a pendulum impact machine that has been suitably instrumented with transducers so that force, velocity, and input energy as a function of contact time can be calculated. The drop weight test utilizes a specimen with a brittle weld crack starter and is used to define the nil-ductility temperature (NDT), the temperature below which the fracture resistance is so low that brittle plane strain cleavage fractures can be initiated dynamically from small flaws. The standard definition of the NDT temperature from the drop weight test has been shown to correspond to a ratio of K_{Id}/σ_{yd} of about 0.5 $\sqrt{\text{in.}}$ This implies that specimens less than about 5/8-inch thick can not be used to establish fracture toughness values corresponding to the NDT temperature. Increased load rate increases the NDT, and thus it is necessary that design data be based upon standard drop weight tests which simulate operational dynamic loading rates.

The dynamic tear test specimen contains a sharp crack-like stress concentrator which has been deliberately embrittled by pressing a hard indentor into the notch. In its usual application, the dynamic tear test parameter is total fracture energy, analogous to that obtained from the Charpy impact test.

However, since the unbroken ligament is much larger in the dynamic tear specimen, fracture propagation energy is a larger fraction of the total energy for the dynamic tear specimen than for the Charpy specimen. For this reason the dynamic tear test is considered to be a more meaningful measure of dynamic toughness than the Charpy test, and is receiving greater acceptance within the Navy community. Also, the dynamic tear specimen can be precracked and the test equipment instrumented in order to provide test data analogous to that obtained in the instrumented Charpy test.

In order to develop improved ship structural design criteria it is necessary that the definition of "dynamic" loading be made more precise so that material property data can be developed based on rational requirements. As suggested above, yield strength, nil-ductility temperature, and fracture toughness all depend upon the speed with which the test is conducted. It is, therefore, reasonable to look for load rates corresponding to actual ship primary structure loading conditions in order to fix the notion of "dynamic" more precisely.

A good recent review of the subject of ship dynamic loadings has been given by Lewis and Zubaly.[9] The vibratory modes of hull-girder response are created by cyclic loads (such as wave excitation) and transient loads (slamming and whipping). The authors have shown that the transient loadings are of significantly higher frequency than are the cyclic loadings, and the two can therefore be considered separately. The phasing is such that slam response seldom adds significantly to initial sagging bending moments, but the whipping that follows always adds to the first hogging moment.

Data recorded from measurements reported by Lewis and Zubaly and others show that the hull girder response of large ships to wave excitation is essentially that of a rigid body and produces bending stresses having a cyclic character with frequencies on the order of 0.1 Hz. Slamming produces primarily a two-noded hull vibration (whipping or springing) that is transient in nature with frequencies of the order of 0.7 Hz for large ships. For observed whipping stresses of about 20 ksi, the corresponding strain rate is about $5\text{-}10 \times 10^{-3}$ sec^{-1}. Dynamic loading rates due to slamming per se, as measured by pressure rise time, may be as much as 10 times those for whipping or springing. These rates are not considered high by normal impact testing technology standards where "dynamic" strain rates refer to rates in excess of about 100/sec.

II. SPECIMEN FABRICATION

A. Ship Plate

A total of twelve heats of ship steel plate were chosen for specimen fabrication. These heats are selected to represent typical samples of ordinary strength, quenched and tempered, and high strength-low alloy ship steels having yield strengths ranging from 40-100 ksi. Although it was desired that all plate be one inch thick, considerations of availability and timing imposed certain compromises. Most of the plate was obtained from Armco Steel Company in Houston. Two small plates of ABS-B were obtained before this project was initiated through the Naval Research Laboratory, which declared these plates excess. Table 1 provides a summary of the heats used in this program.

A chemical analysis of samples from the twelve plate heats was conducted by Armco Steel. This analysis served not only to verify the Armco certification reports but also to assure the composition of the two heats of ABS-B obtained through the NRL. Table 2 summarizes the results of that analysis.

All heats were within the specified chemistry except for one. The ABS-CS had a manganese content of 1.42 vs 1.35 maximum allowable. All other elements for all materials fit either the applicable ASTM or ABS requirements. Regarding the required tensile properties, there were two exceptions. The AH-32 exceeds the maximum allowable tensile strength of 85 ksi by 5 ksi; the yield and the elongation are acceptable. The other exception is one heat of A517; here the elongation is 13.6 percent, or slightly below the 16 percent value specified by ASTM.

Other properties, particularly the Charpy and NDT values, are more difficult to assess. For example, the NDT for ABS-B was found to be 50-60°F in this investigation. While this is higher than some other investigators have found, it should be noted that among four sources[1, 2, 14] including this program, a spread of 60°F is reported between the highest and lowest NDT values. On the other hand, for ABS-CS material, three investigations including this one also report a spread of 60°F in the NDT. Sizable heat-to-heat variation can also be cited for Charpy and dynamic tear results. Thus, without a large data base of material properties from which to draw, it is very difficult to specify typical properties for a material, particularly when the test itself involves a degree of uncertainty as, e.g., in the Charpy test.

B. Fabrication Of Tensile Specimens

Tensile specimens were fabricated as 0.250-inch diameter round specimens having a nominal gage length of 1.25 inch

Table 1. Summary of Steel Plate Received

Material	SwRI Heat No.	Supplier's Heat No.	Thickness	Size*	Source
ABS-DS	1	66359	1"	$\overline{24}$" × 96"	Armco
ABS AH-32	2	65769	1"	$\overline{24}$" × 96"	Armco
ABS EH-32[a]	3	66340	1"	$\overline{120}$" × 96"	Armco
ABS-CS[a]	4	80635	1"	$\overline{192}$" × 96"	Armco
ASTM A517-D[b]	5	48784	1"	$\overline{18}$" × 84"	Armco
ASTM A517-D[b]	6	37098	1-1/4"	$\overline{120}$" × 84"	Armco
ASTM A678-C[b]	7	41911	1-3/8"	$\overline{18}$" × 74"	Armco
ASTM A678-C[b]	8	63149	1-1/4"	$\overline{144}$" × 84"	Armco
ASTM A537-B[b]	9	66144	1"	$\overline{18}$" × 84"	Armco
ASTM A537-B[b]	10	48434	1"	$\overline{138}$" × 96"	Armco
ABS-B[c]	11	?	1"	$\overline{36}$" × 24"	Todd/NRL
ABS-B[c]	12	432K3581	1"	$\overline{36}$" × 24"	Bethlehem/NRL

* bar indicates rolling direction
(a) Normalized
(b) Q & T
(c) Semi-killed

Table 2. Results of Chemistry and Hardness Tests of Plate Samples Submitted by Southwest Research Institute

	Material	Probable Heat Number	Thickness	Brinell Hardness	Wet C	Mn	P	Wet S	Si	Cr	Ni	Mo	Cu	Ti	V	B	C
	ABS DS	66359	1.029"	134	.10	1.07	.010	.015	.21	.13	.13	.02	.09	Nil	Nil	Nil	N
	AH-32	66769	1.010"	183	.18	1.16	.012	.024	.26	.11	.07	.03	.11	Nil	.044	Nil	N
	EH-32	66340	1.026"	149	.16	1.27	.010	.025	.22	.12	.09	.03	.09	Nil	.042	Nil	Ni
	ABS CS	80635	1.013"	143	.11	1.42	.016	.026	.34	.13	.04	.02	.03	Nil	Nil	Nil	Ni
	A517, D	48748	1.041"	262	.18	.61	.012	.022	.18	1.12	.19	.21	.30	.095	Nil	.002	Ni
	A517, D	37098	1.292"	255	.18	.55	.011	.012	.27	.98	.09	.20	.24	.101	Nil	.003	Ni
	A678, C	41911	1.421"	217	.20	1.44	.010	.027	.45	.22	.22	.06	.13	Nil	Nil	Nil	Ni
	A678, C	63149?	1.302"	202	.19	1.55	.010	.013	.47	.18	.19	.07	.08	Nil	Nil	Nil	Ni
	A537, B	66144	1.058"	159	.15	1.20	.010	.021	.40	.23	.13	.04	.08	Nil	Nil	Nil	Ni
0	A537, B	48434	1.016"	174	.17	1.32	.010	.019	.33	.21	.25	.06	.14	Nil	Nil	Nil	Ni
1	ABS B	?	1.018"	121	.18	1.04	.010	.020	.03	.01	Nil	Nil	.03	Nil	Nil	Nil	Ni
2		?	1.018"	126	.17	.97	.020	.033	Nil	.01	Nil	Nil	.01	Nil	Nil	Nil	Ni

according to ASTM E-8. This specimen is proportional in scale, but smaller in size, to the standard ASTM 0.505-inch diameter Round Tension Test Specimen. The ends of the specimens were threaded to 1/2-13NC-2A for use with the grips in the Instron testing machine. All these specimens were taken with the long dimension in the rolling direction of the plate, from a cylinder whose axis was at the 1/4 T thickness position. While this specimen is smaller than would be normally used for 1 inch thick plate, it was chosen to match the size and location of the corresponding tensile specimens in the companion study, SSC-276.[3] The slightly longer gage length, 1.25 vs 1.00 inches, was chosen for convenience in applying instrumentation.

C. Fabrication Of Dynamic Tear Specimens

The dynamic tear (DT) specimen test procedure is presently (1976) proposed as an ASTM standard. The specimen is a single edge notched beam 7.125 inches in length, 0.625 inch in thickness, and notched and mid-span to a depth of 0.475 inch, where the total specimen width is 1.60 inches. The specimen is normally tested in a double pendulum type machine, and is dynamically loaded in three-point bending, on supports placed 6.5 inches apart, by a striker tup of radius 0.5 inch so as to place the notch in Mode I tension loading. Total energy loss during separation is recorded. For purposes of the present investigation DT specimens were also loaded similarly in conventional testing machines at slower loading rates. Details of the test specimen and test procedure may be found in Reference (11).

Specimens were machined in the L-T orientation (Figure 1) from the plate surface. The specimens were all fatigue precracked. This precracking operation was accomplished in three point bending cyclic loading at 23 Hz with a maximum centerpoint load/cycle of 4500 lbs. This cyclic loading was sufficient to create a crack of about .060 to .120 inch, visible from both ends, in approximately 5 x 10^4 cycles.*

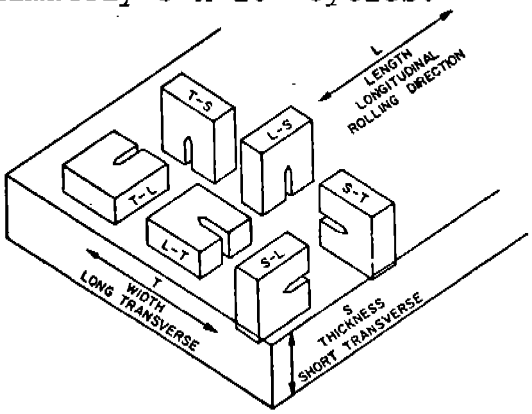

Figure 1. Specimen Orientation Code

*The specimens were subjected to from 22,000 to 145,000 cycles of load.

III. TEST MATRIX AND TEST PROCEDURES

A. Test Matrix

Table 3 presents a summary of the numbers and kinds of tests as related to each of the heats tested. As indicated some of the test data were drawn from the report SSC-276 (3) which serves as a companion to the present report, in order to have as complete a basis as possible for evaluating load rate and temperature effects on yield strength and toughness as measured by the dynamic tear specimen. Only eleven of the twelve available heats were tested in the present program; Heat Number 12, ABS B, is carried in the table for consistency with the heat designations of Report SSC-276, in which Heat Number 12 was used in the test program. In the test data to be reported, minor deviations from this test matrix can be found. These deviations are present in a few of the DT tests, where in some cases fewer than six tests were sufficient to define the upper and lower shelf energy levels and their respective temperatures.

B. Tensile Testing

Tension tests were conducted at various head (strain) rates and temperatures in accordance with the test matrix, Table 3. Two head rates were used: dynamic (0.10 in/sec) and impact (approximately 6.0 in/sec). The dynamic tests were conducted in a closed loop mode on a 22 KIP MTS electro-hydraulic universal testing machine. The impact tests were conducted in the same facility, but in the open loop mode to achieve the maximum head rate possible. A head displacement transducer, part of the testing machine, was used to determine strain, and a load-strain curve was plotted out for each test to enable upper and lower yield point, and ultimate strength, to be determined. Elongation was determined from two reference marks inscribed on the specimen. Data at static head rates (1.67×10^{-4} in/sec) was taken from Report SSC-276 (3) to provide a more complete data base. A complete data summary is given in Table 4.

Testing at temperatures below ambient was accomplished by surrounding the specimen with a container filled with a mixture of methanol and dry ice. The specimen was allowed to stabilize at the test temperature, and the test was conducted with the specimen remaining immersed in the bath. A thermocouple was attached to the gage section, under the methanol/dry ice solution to monitor the temperature. Testing above room temperature was accomplished by stabilizing the specimen in a water bath warmed by a submersible heater, and testing with the specimen immersed in the warm bath.

C. Dynamic Tear Testing

Five-eighths-inch dynamic tear specimens were tested in

Table 3. Overall Test Matrix

TEST TYPE	HEAT NUMBER (SEE KEY)											
	1	2	3	4	5	6	7	8	9	10	11	12
Tension Rate (Static) [1]	-	1	1	1	1	1	1	1	1	1	1	-
Tension Rate (Dynamic & Impact) [2]	2	2	6	6	2	6	2	2	2	2	2	-
DT, 5/8", Precrack (L-T) [3]	36	6	36	36	6	36	6	6	6	6	6	-
DT, 5/8", Press-Notch (L-T) [1]	-	6	6	6	6	6	6	6	6	6	6	-

KEY

Heat No.	Material
1	ABS-DS
2	ABS AH-32
3	ABS EH-32
4	ABS CS
5	ASTM A517-D
6	ASTM A517-D
7	ASTM A678-C
8	ASTM A678-C
9	ASTM A537-B
10	ASTM A537-B
11	ABS B
12	ABS B

NOTES

[1] Data drawn from SR-224 study (3)

[2] Heats 1, 2, 5, 7, 8, 9, 10, 11: 2 temperatures (0°F, 75°F) at dynamic head rate = 0.10 in/sec

Heats 3, 4, 6: 3 temperatures (75°F and 2 others) at dynamic (0.10 in/sec) and impact (6.0 in/sec) head rates

[3] Heats 2, 5, 7, 8, 9, 10, 11: 6 temperatures (0°F, 75°F and 4 others) at dynamic heat rate = 1.0 in/sec

Heats 1, 3, 4, 6: 6 temperatures (0°F, 75°F and 4 others) at static (4×10^{-3} in/sec), dynamic (1.0 in/sec), and DT impact head rates; duplicate tests

Table 4. Tensile Test Results

Heat No.	Material	Head Rate (in/sec)	T, °F	Initial Dia (in)	Initial Gage Length (in)	Final Dia (in)	Final Gage Length (in)	Lower Yield $\sigma_{\ell y}$ (ksi)	Upper Yield σ_{uy} (ksi)	Ultimate Strength σ_u (ksi)
(1)	ABS DS	0.10	0	0.2502	1.219	0.1332	1.568	49.8	51.6	70.3
		0.10	75	0.2535	1.176	0.1300	1.610	42.1	51.0	66.3
(2)	ABS AH-32	1.67×10^{-4}	75	0.2507	1.278	0.1590	1.558	58.4	64.6	86.4
		0.10	0	0.2486	1.203	0.1498	1.540		72.4	
		0.10	0	0.2525	1.128	0.1525	1.390		76.3	93.3
		0.10	75	0.2546	1.220	0.1566	1.565	60.4	68.3	88.4
(3)	ABS EH-32	1.67×10^{-4}	75	0.2489	1.253	0.1310	1.612	50.6	51.5	73.9
		0.10	-80	0.2542	1.170	0.1452	1.584		84.6	86.1
		0.10	0	0.2547	1.145	0.1400	1.538		75.0	79.4
		0.10	75	0.2552	1.169	0.1388	1.539	52.7	64.9	75.2
		6.06	-80	0.2506	1.246	0.1473	1.606		90.8	90.3
		6.11	0	0.2507	1.253	0.1451	1.630		89.1	84.0
		6.00	75	0.2541	1.204	0.1418	1.612	57.2	79.4	79.9
(4)	ABS CS	1.67×10^{-4}	75	0.2492	1.281	0.1400	1.657	47.3	48.0	69.0
		0.10	-80	0.2552	1.228	0.1376	1.658		83.5	81.1
		0.10	0	0.2552	1.181	0.1275	1.620		73.2	75.2
		0.10	75	0.2553	1.178	0.1301	1.608	50.3	59.1	69.8
		6.15	-80	0.2490	1.162	0.1355	1.502		83.2	86.2
		6.14	0	0.2499	1.240	0.1355	1.644		83.7	78.6
		6.11	75	0.2506	1.221	0.1316	1.701	54.8	73.0	74.0
(5)	ASTM A517-D	1.67×10^{-4}	75	0.2477	1.279	0.1390	1.471	120.6	120.6	126.7
		0.10	0	0.2505	1.227	0.1441	1.445		130.3	131.9
		0.10	75	0.2505	1.178	0.1438	1.388	117.7	118.7	124.8
(6)	ASTM A517-D	1.67×10^{-4}	75	0.2516	1.284	0.1490	1.458	128.2	128.2	134.6
		0.10	0	0.2547	1.185	0.1560	1.384		138.7	141.2
		0.10	75	0.2504	1.217	0.1515	1.410	125.0	126.0	133.1
		0.10	160	0.2520	1.239	0.1519	1.439		128.3	130.8
		5.58	-80	0.2511	1.226	0.1346	1.457		155.6	152.5
		5.71	0	0.2508	1.197	0.1616	1.398		141.7	144.7
		5.67	75	0.2545	1.213	0.1573	1.427	129.7	133.6	138.5
		5.88	160	0.2510	1.125	0.1538	1.305		126.3	132.8
(7)	ASTM A678-C	1.67×10^{-4}	75	0.2474	1.276	0.1340	1.530	73.8	77.9	96.3
		0.10	0	0.2546	1.185	0.1400	1.485		93.3	105.6
		0.10	75	0.2505	1.189	0.1395	1.453	77.1	80.6	99.9
(8)	ASTM A678-C	1.67×10^{-4}	75	0.2487	1.268	0.1320	1.560	76.9	86.2	96.3
		0.10	0	0.2545	1.178	0.1508	1.459		95.3	103.6
		0.10	75	0.2508	1.205	0.1282	1.492	77.9	84.0	98.2
(9)	ASTM A537-B	1.67×10^{-4}	75	0.2527	1.275	0.1290	1.654	62.8	67.0	83.7
		0.10	0	0.2555	1.202	0.1349	1.532		85.8	89.7
		0.10	75	0.2552	1.192	0.1313	1.507	64.5	71.8	84.0
(10)	ASTM A537-B	1.67×10^{-4}	75	0.2484	1.260	0.1390	1.546	67.9	75.3	89.6
		0.10	0	0.2502	1.225	0.1405	1.524		88.4	94.7
		0.10	75	0.2507	1.209	0.1450	1.514	72.4	80.5	91.1
(11)	ABS B	1.67×10^{-4}	75	0.2496	1.267	0.1460	1.673	34.8	37.9	63.9
		0.10	0	0.2551	1.204	0.1545	1.602		64.1	70.5
		0.10	75	0.2546	1.182	0.1511	1.605	39.8	47.6	66.3

NOTE: All data at static head rate (1.67 x 10^{-} in/sec) drawn from SR-224 study.[3]

two different machines. Impact-rate tests were conducted in a 2000 ft-lb capacity Mark II dynamic tear test machine, having a double pendulum arrangement. This machine is calibrated periodically using a static moment technique. Additionally, it is checked each day before a test series is conducted by letting the pendula swing freely through one complete cycle, then checking that the dial indicator reads zero ft-lbs energy. Static and dynamic rate tests were conducted in a 50 Kip servo-controlled MTS universal testing machine. Fixturing was provided so as to load the specimen in 3-point bending similar to the loading produced by the DT machine. The distance between the two support points as fixtured for these tests was 6.75 inches, whereas the corresponding support distance for the DT machine is 6.5 inches. Thus, the force-moment relationship in the two cases differs by the factor 1.0385.

Specimens were temperature conditioned in the same way as were the tensile specimens, described in Section III.B. Specimens were cooled by immersing them in an agitated bath of methanol and dry ice, and held at temperature for 20 minutes. Elevated temperature testing was accomplished by stabilizing the specimens in an agitated bath of water warmed by submersible heaters. For impact testing in the DT machine the specimen was taken from the bath, placed in the machine and immediately tested; total elapsed time from the bath to test completion was 10 seconds or less. For static and dynamic testing the specimen was kept immersed in a container of the cooled or warmed fluid during the test.

Most of the DT testing involved determining total energy to fracture the specimen. In the case of the DT machine, the energy-to-fracture is read out directly on a calibrated dial indicator. In the case of the static and dynamic tests, the load deflection curve was automatically plotted out during the test from load cell and head rate inputs. Then, the area under the load deflection curve was determined by digitizing the curve and integrating by a quadrature routine to determine energy.

A few of the tests were carried out with the specimen itself instrumented as well, to provide information leading to the evaluation of a fracture toughness. In order to do this, a specimen crack opening displacement (COD) gage was designed and developed especially for the DT specimen.

The COD gage is a capacitance type gage which mounts across the notch in the DT specimen on the face opposite to the impact face, Figure 2. It consists of two simple assemblies. One contains the active capacitance plates and is mounted by two screws on one side of the notch. The other carries a grounded slide plate and is mounted by a third screw on the other side of the notch. The first assembly is composed of two brass pieces, each with a brass sensing element encapsulated in epoxy. When the two halves are assembled, the two sensing elements form a parallel plate capacitor with an air gap between them. The sensing elements are surrounded on all sides, except at the gap opening, by the brass shell pieces. The second assembly is laminated from two brass blocks and the brass slider plate. The blocks support the thin slider plate and guide it into the gap between the sensing plates.

When the COD gage is mounted on the DT specimen, as shown in Figure 2, the shell of the first assembly and the entire second assembly are connected to instrument ground through the specimen. The capacitance between the sensing elements is then limited to that gap area, or window, which is not covered by the slider plate. As the specimen is deformed during a test, the slider is drawn from the gap and the capacitance increases proportionately as the window area increases.

The minute change in capacitance produced by movement of the slider can be measured only with very sensitive instrumentation capable of separating the capacitance between the sensing elements from capacitance between each element and ground. In addition, the frequency response of the instrumentation must be adequate for the impact tests. Capacitance instrumentation was developed at SwRI for these tests. The active element in the COD gage is one arm of a capacitance bridge. The bridge is driven with a carrier from a low impedance source, and the output of the bridge is at virtual ground so that the effect of capacitance to ground is minimized. The instrumentation was modified for these tests to operate with a carrier frequency of 100 kHz to give adequate high-frequency response.

In addition to the COD gage, specimen instrumentation, where applicable, consisted also of a strain gage mounted on the specimen to measure the specimen response in the region near the crack tip. Several different locations were used for placing the strain gages, as shown in Figure 3. The strain gage was placed only on the instrumented specimens tested at room temperature, since the force-time data from the tup and the strain-time data were essentially coincident except for a time-delay shift. Since the strain gage was judged to produce no extra data, it was dropped from all non-ambient tests.

The DT machine was also fitted with an instrumented tup to enable the force-time relationship of the impact event to be determined. This instrumentation consisted of an elastic element incorporating a semiconductor full Wheatstone bridge to record dynamic loads. The bandwidth for this element is -3 dB at 20 kHz.

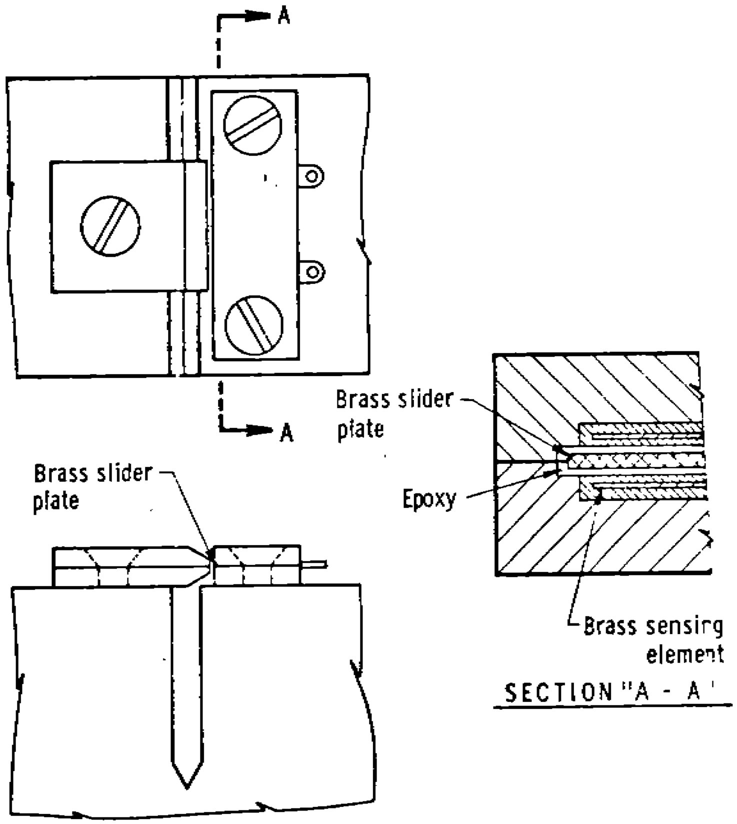

Figure 2. Capacitance-Type COD Gage

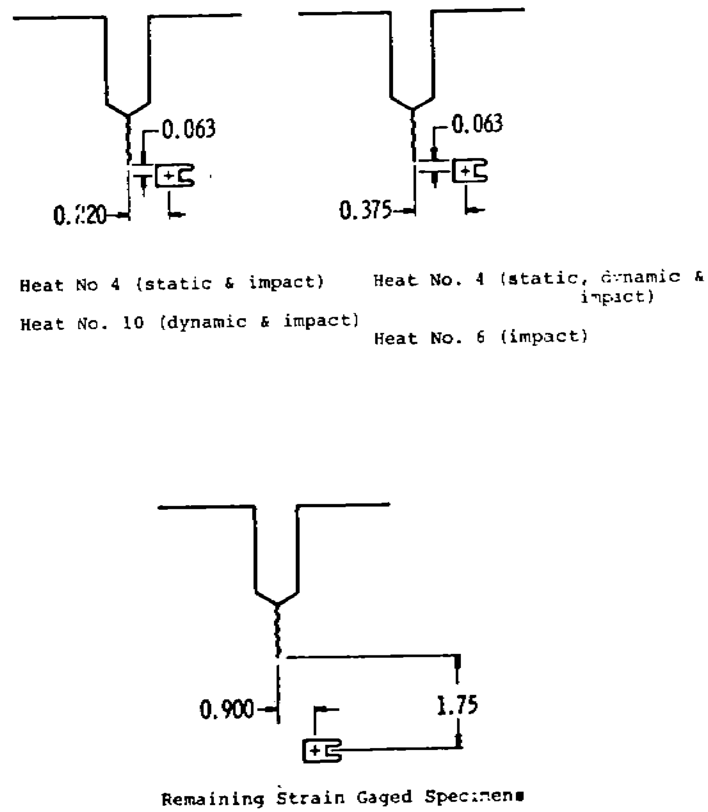

Figure 3. Strain Gage Locations for DT Specimens (All conducted at 75° F)

IV. TEST RESULTS

A. Tensile Rate Test Data

The relationship between yield strength, temperature, and strain rate is often expressed mathematically by an Arrhenius relation derived from rate process theory. One commonly-used expression[12,13] is a more general form of the rate parameter, R, discussed previously [7,8]; this expression is:

$$\dot{\varepsilon} = \dot{\varepsilon}_0 \exp - \left[\frac{U - (\sigma_y - \sigma_i)\, V}{kT}\right] \tag{1}$$

in which $\dot{\varepsilon}$, σ_y , and T are, respectively, the strain rate, yield strength, and absolute temperature. The other parameters entering into Eq. (1) are

$\dot{\varepsilon}_0$ = a viscosity coefficient, having the same dimensions as $\dot{\varepsilon}$, which is a function of the dislocation density, Burger's vector, and dislocation velocity (and hence plastic strain). For steel alloys $\dot{\varepsilon}_0 \approx 10^{12}$/sec, but may vary with microstructure and deformation history.

U = activation energy, of the order 1 eV = 1.418×10^{-18} in-lb.

σ_i = long range "athermal" stress field opposing dislocation motion; also, high-temperature elastic limit.

V = activation volume, typically 10-100 b^3, where b, the Burger's vector, is $\approx 3\text{Å} = 1.18 \times 10^{-8}$ in.

k = Boltzmann's constant, 6.786×10^{-23} in-lb/°R.

Equation (1) can be rearranged to give the yield strength explicitly:

$$\sigma_y = \sigma_0 - \frac{kT}{V} \ln (\dot{\varepsilon}_0/\dot{\varepsilon}) \tag{2}$$

where $\sigma_0 = \sigma_i + U/V$. This expression shows that the yield strength decreases linearly with (absolute) temperature, and increases logarithmically with strain rate.

In applying Eq. (2), it should be noticed that as the temperature approaches absolute zero, then $\sigma_y = \sigma_0$; hence σ_0 has the interpretation of the yield strength at absolute zero temperature, and $\sigma_0 > \sigma_y$. The activation volume V can be calculated from the change of σ_y with strain rate or temperature. By taking the respective partial derivatives one finds

$$V = \frac{k \ln (\dot{\varepsilon}/\dot{\varepsilon}_0)}{\partial\sigma_y/\partial T} \tag{3a}$$

or

$$V = \frac{kT}{\dot{\varepsilon}\ (\partial\sigma_y/\partial\dot{\varepsilon})} = \frac{kT}{\partial\sigma_y/\partial\ \ell n\ \dot{\varepsilon}} \tag{3b}$$

and thus

$$T\frac{\partial\sigma_y}{\partial T} = \dot{\varepsilon}\ \ell n\ (\dot{\varepsilon}/\dot{\varepsilon}_o)\frac{\partial\sigma_y}{\partial\dot{\varepsilon}} = \ell n\ (\dot{\varepsilon}/\dot{\varepsilon}_o)\ \frac{\partial\sigma_y}{\partial\ \ell n\ \dot{\varepsilon}} \tag{4}$$

In calculations of V using experimental data, Eq. (3b) is preferred since it does not contain the parameter $\dot{\varepsilon}_0$. If this is used, then Eq. (4) can be used to determine $\dot{\varepsilon}_0$:

$$\dot{\varepsilon}_o = \dot{\varepsilon}\ \exp - \left[\frac{T\ (\partial\sigma_y/\partial T)}{\dot{\varepsilon}\ (\partial\sigma_y/\partial\dot{\varepsilon})}\right] = \dot{\varepsilon}\ \exp - \left[\frac{T\partial\sigma_y/\partial T}{\partial\sigma_y/\partial\ \ell n\ \dot{\varepsilon}}\right] \tag{5}$$

Since V and $\dot{\varepsilon}_0$ may now be considered known from the data, σ_y can be calculated directly from Eq. (2).

These expressions are often used to represent data on the strain rate and temperature dependence of the flow (yield) stress for polycrystalline metals. They are especially useful in describing the flow characteristics of pure metals, or those having simple microstructures. For complex metals, such as quenched and tempered ship steels having martensitic microstructures, the physical arguments on which these equations are based frequently fail to describe real flow processes in detail. Nevertheless, they do illustrate how yield stress is linearly related to absolute temperature and to the logarithm of strain rate; representations of σ_y as a function of T and of $\ell n\ \dot{\varepsilon}$ are sufficient to describe flow behavior.

Table 4 presents the experimental data on uniaxial tension tests on specimens from Heats 1-11. Three strain rates were chosen to represent the range in load rates that may be encountered in primary ship structure service. For the sake of simplicity, these rates will be referred to as

Load Rate	Cross-Head Velocity	Strain Rate (in/in/sec)
Static	0.01 in/min	$\approx 1.3 \times 10^{-4}$
Dynamic	0.10 in/sec	≈ 0.08
Impact	≈ 6 in/sec	$\approx 5.$

Tests on Heat No. 2 (AH-32) were conducted only at the dynamic rate. All other heats were tested at both static and dynamic rates, and in the case of Heats 3 (EH-32), 4 (CS), and 5 & 6 (A517-D), impact tests were also conducted.

Tension stress-strain tests were conducted at various temperatures as well. All heats were tested at both 0°F and 75°F, and, in addition, were tested at higher and lower temperatures as appropriate. Details are provided in Table 4.

Most of the materials tested exhibited both an upper and a lower yield strength; for purposes of data analysis to determine the slope $\partial \sigma_y/\partial T$, upper yield strength values were used. In several cases only two data points were available from which to determine $\partial \sigma_y/\partial T$. Owing to the normal scatter inherent in yield strength determination, the calculated slopes in these cases must be considered only approximate. Table 5 summarizes the σ_y vs T slopes determined in this manner. In the three cases (Heats 3, 4, and 6), where comparative results were available for dynamic and impact load rates, the absolute values of $\partial \sigma_y/\partial T$ for impact test conditions were less than those values obtained under dynamic conditions. This finding agrees with Eq. (3a), which indicates that $\partial \sigma_y/\partial T \approx \ell n\ (\dot{\varepsilon}/\dot{\varepsilon}_o)$.

Upper yield strength values were also used to assess the dependence of yield strength σ_y on $\ell n\ \dot{\varepsilon}$. As before, in many cases there is a paucity of data available from which to calculate the slope $\partial \sigma_y/\partial \ell n\ \dot{\varepsilon}$ with confidence. These calculations are made more imprecise due to the sensitivity of the $\sigma_y - \ell n\ \dot{\varepsilon}$ relationship to normal scatter in determining yield strength. Table 6 summarizes the results of these calculations. Several of the values of $\partial \sigma_y/\partial\ \ell n\ \dot{\varepsilon}$ are seen to be negative; these data are probably invalid and are caused by the lack of sufficient data to make realistic determinations possible. The same can be said of those values of $\partial \sigma_y/\partial\ \ell n\ \dot{\varepsilon}$ which are positive, but small. Such values imply $\dot{\varepsilon}_o$ [Eq. (5)] to be very large, several orders of magnitude greater than the range 10^{10} to 10^{14} generally reported.

The mathematical model discussed above and presented as Eq. (2) can be used to determine the relation between the "dynamic" (or, more properly, the "impact") yield strength σ_{yd} and the conventional "static" yield strength σ_{ys} . To do this, it is convenient to define the static yield strength mathematically in terms of the dynamic yield strength:

$$\sigma_{ys} = \sigma_{yd}\Bigg|_{\substack{\dot{\varepsilon} = \dot{\varepsilon}_s = 10^{-4} \\ T = T_s = 75°F}} \tag{6}$$

The "static" strain rate has been chosen arbitrarily as 10^{-4} in/in/sec as representative of conventional test data. Then, σ_{yd} can be computed as

Table 5. Summary of Slopes of Yield Strength-Temperature Results

Heat No.	Material	Load Rate	$\partial\sigma y/\partial T$ (lb/in^2/°F)
2	AH-32	Dynamic	-100.
3	EH-32	Dynamic	-125.
3	EH-32	Impact	- 95.
4	CS	Dynamic	-154.
4	CS	Impact	-119.
5	A517-D	Dynamic	-158.
6	A517-D	Dynamic	-158.
6	A517-D	Impact	-119.
7	A678-C	Dynamic	-168.
8	A678-C	Dynamic	-150.
9	A537-B	Dynamic	-190.
10	A537-B	Dynamic	-105.
11	B	Dynamic	-219.

Table 6. Summary of Slopes of Yield Strength-Strength - Log $\dot{\varepsilon}$ Results

Heat No.	Material	Temperature, °F	$\partial\sigma y/\partial \ln \dot{\varepsilon}$
2	AH-32	75	625.
3	EH-32	-80	1579.
3	EH-32	0	3333.
3	EH-32	75	2632.
4	CS	-80	0.
4	CS	0	2500.
4	CS	75	2381.
5	A517-D	75	- 304.
6	A517-D	0	790.
6	A517-D	75	1053.
6	A517-D	160	- 526.
7	A678-C	75	304.
8	A678-C	75	- 391.
9	A537-B	75	769.
10	A537-B	75	833.
11	B	75	1539.

$$\sigma_{yd} = \sigma_{ys} + (\sigma_{yd} - \sigma_{ys}) \tag{7}$$

which, with Eq. (2), reduces to

$$\sigma_{yd} = \sigma_{ys} + \frac{kT}{V}\left[\frac{T_s}{T}\,\ell n\,(\dot{\varepsilon}_o/\dot{\varepsilon}_s) - \ell n\,(\dot{\varepsilon}_o/\dot{\varepsilon})\right] \tag{8}$$

The second term on the right hand side represents the amount of increase (or decrease) in the static yield strength due to temperature and strain rate effects. At room temperature $T = T_s$, Eq. (8) gives

$$\sigma_{yd} = \sigma_{ys} + \frac{kT_s}{V}\,\ell n\,(\dot{\varepsilon}/\dot{\varepsilon}_s) \tag{9}$$

which reveals the effect of strain rate on room temperature yield strength.

In the analysis of the present data it is assumed that σ_{yd} refers to yield strength at strain rates characteristic of the dynamic tear (DT) test. Analysis of the instrumented DT tests reported herein suggests that the flow stress is reached in approximately 200 μ sec. The flow strains are on the order $\sigma_y/E \approx 3 \times 10^{-3}$ for the strength range tested in this program. Thus, the strain rate $\dot{\varepsilon}$ for the DT test can be estimated as of the order $3 \times 10^{-3}/200 \times 10^{-6} = 15$ in/in/sec. The calculation of $\dot{\varepsilon}_0$ is more speculative; however, most of the present data show $\dot{\varepsilon}_0$ to be of order 10^{12}, and this value will be assumed to be constant for all heats used in this program. Then, $\ell n\,(\dot{\varepsilon}_0/\dot{\varepsilon}) = 25$ for DT impact strain rates, so that Eq. (8) reduces to

$$\sigma_{yd} = \sigma_{ys} + 36.84\,\frac{kT}{V}\left(\frac{T_s}{T} - 0.6786\right) \cong \sigma_{ys} + \sigma'_y \tag{10}$$

Equation (10) shows that the dynamic yield strength is equal to the static yield strength, σ_{ys} , plus a dynamic overstress, σ'_{yd}, which is temperature-dependent. In order to make calculations of σ_{yd} it is necessary to determine the activation volume V. Calculations of V were made from Eq. (3b), and the results, while scattered, indicated that all heats tested can be grouped into three categories, within which V can be assumed constant:

Heats	Materials	V(in^3)
1- 4	DS, AH-32, EH-32, CS	1.3×10^{-23}
5-10	all ASTM	4.0×10^{-23}
11-12	B	2.4×10^{-23}

This grouping is consistent also from metallurgical considerations, inasmuch as they represent predominantly bainite, martensite, and ferrite microstructures, respectively.

Table 7 presents the calculated values of σ_y' in Eq.(10) for dynamic yield strength for various temperatures. At low temperatures, σ_y' is high, owing to the strain rate effect, but decreases with thermal softening at higher temperatures. Equation (10) predicts a temperature of 328°F at which all material heats have the same dynamic (DT-impact) yield strength as they do at 75°F under quasi-static loading. At this temperature, the competing mechanisms of strain rate and temperature balance.

The calculations used to develop Table 7 depend upon the value of $\dot{\varepsilon}_0$, which entered into Eq. (8) and hence into Eq. (10). Although the value chosen for $\dot{\varepsilon}_0$ is somewhat judgemental in view of the paucity of data, it is comforting to know that the numbers given in Table 7 are rather insensitive to $\dot{\varepsilon}_0$. Varying $\dot{\varepsilon}_0$ by an order of magnitude either side of the chosen value of 10^{12} alters the values in the table generally by less than 6%. At $T=T_s=75°F=535°R$, of course, σ_y' is independent of $\dot{\varepsilon}_0$. Moreover, varying $\dot{\varepsilon}_0$ by an order of magnitude changes the calculated temperature of 328°F (at which the dynamic yield strength is the same as for static loading at 75°F) by about +32°F (at $\dot{\varepsilon}_0 = 10^{11}$) and -51°F (at $\dot{\varepsilon}_0 = 10^{13}$).

The figures shown in Table 7 indicate that there is a substantial increase in yield strength at room temperature in going from static to impact loading rates. The calculated values, of course, are (inversely) proportional to the activation volume V, which was determined through the experiments. The paucity of data made it difficult to determine V with high confidence. Nevertheless, it appears as though the assumption $\sigma_{yd} = \sigma_{ys} + 20$ ksi in the SSC-244 criterion [1], while perhaps a good average correction, may differ widely from true values for various heats.

B. Dynamic Tear Tests

1. Energy to Failure

Table 8 presents the data for the energy-of-fracture W_f as measured on the precracked dynamic tear (DT) specimens loaded at three different head rates. The test temperatures were selected for each heat in an attempt to define the upper and lower shelves as well as the transition temperature region. These data are plotted in Figures 4 - 14. The figures representing the data for Heats 3, 4, and 6 also contain data for the same kind of specimens having press-notches rather than being precracked; these test data were drawn from Reference 3, and are reproduced in Table 9.

Table 7. Dynamic Overstress σ_y' As a Function of Material Category and Temperature

Heats	Materials	Dynamic Overstress σ_y' (ksi)				
		-80°F	0°F	32°F	75°F	160°F
1 - 4	DS, AH-32, EH-32, CS	53.3	42.9	38.7	33.1	22.0
5 - 10	all ASTM	17.3	13.9	12.6	10.7	7.1
11 - 12	B	28.9	23.2	21.0	17.9	11.9

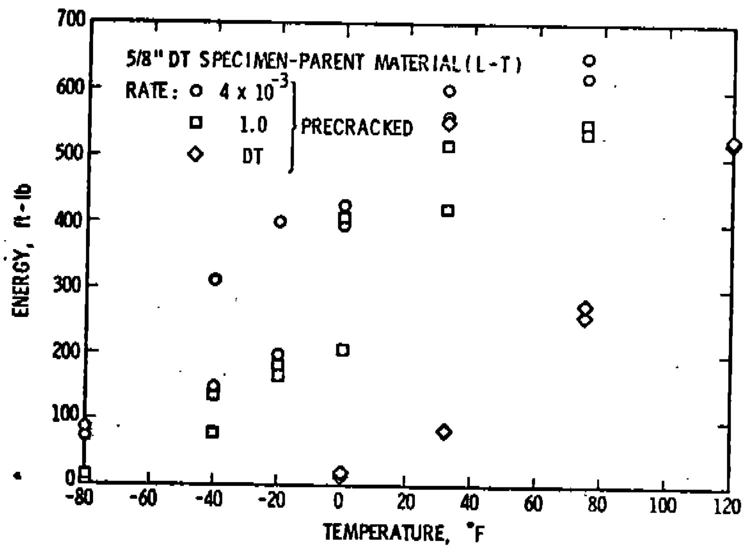

Figure 4. DT Energy, Heat No. 1 (DS)

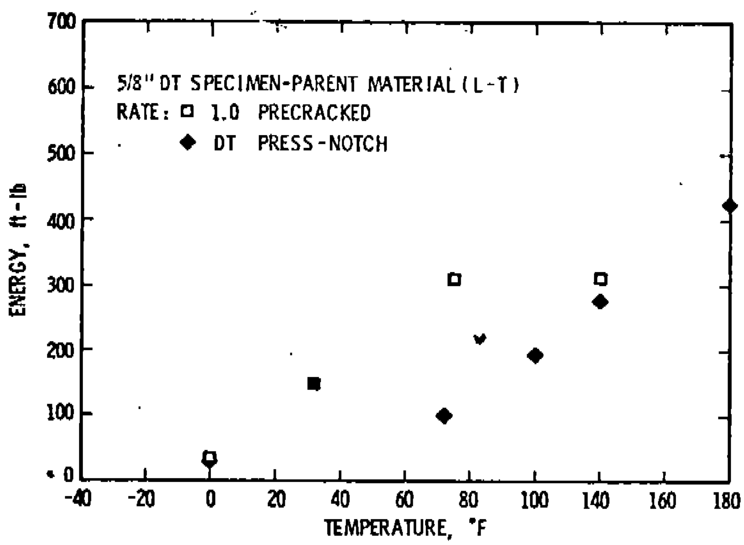

Figure 5. DT Energy, Heat No. 2 (AH-32)

Table 8. 5/8" Dynamic Tear Test Energy Results Precracked L-T Orientation

Heat No.	Material	Head Rate (in/sec)	Ft-Lb Energy Absorbed At Temperature (in °F) -80	-60	-40	-20	0	32	75	120	160
1	ABS-DS	4×10^{-3}	86,74		311,148	402,198	397,428	602,559	651,622		
1	ABS-DS	1.0	13.4,8.		80,468,137	183,167	409,206	442,518	538,551		
1	ABS-DS	DT impact					15,20	85,555	275,260*	525,530	800,880
2	AH-32	1.0					35	148	312	311	
3	EH-32	4×10^{-3}	225,411		422,398	414,439	460,442		435,338		
3	EH-32	1.0	265,440		507,488	505,483	488,484		398,405		
3	EH-32	DT impact				65,75	230,240	530,600	540,570	515,530	
4	ABS-CS	4×10^{-3}	478,442	440,458	445,436	439,421	417,429		486,412		
4	ABS-CS	1.0	234,507	525,477	495,498	450,442	462,487		538,669		
4	ABS-CS	DT impact				96,126	122,112	593,485	605,655		
5	A517-D	1.0	143		156	488	510		425		
6	A517-D	4×10^{-3}			87,49	100,71	106,105	197,137	380,385	357,361	
6	A517-D	1.0			94,49	118,96,123,140	157,159	212,202	399,406	407,404	
6	A517-D	DT impact				60,100	110,115	190,220	335	375,490	380,470
7	A678-C	1.0	571		584		603		656		
8	A678-C	1.0	704		694		680		638		
9	A537-B	1.0	590		620	613	588		510		
10	A537-B	1.0	385		387	407	428		358*		
11	ABS-B	1.0				32	64	491	466		

*A specimen from Heat 10 was inadvertently run at 4×10^{-3} in/sec at 75°F, and registered 199 ft-lbs.

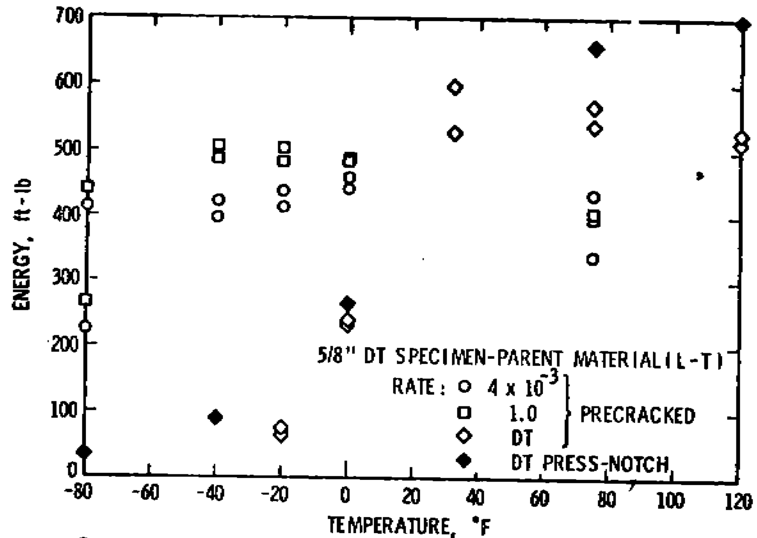

Figure 6. DT Energy, Heat No. 3 (EH-32)

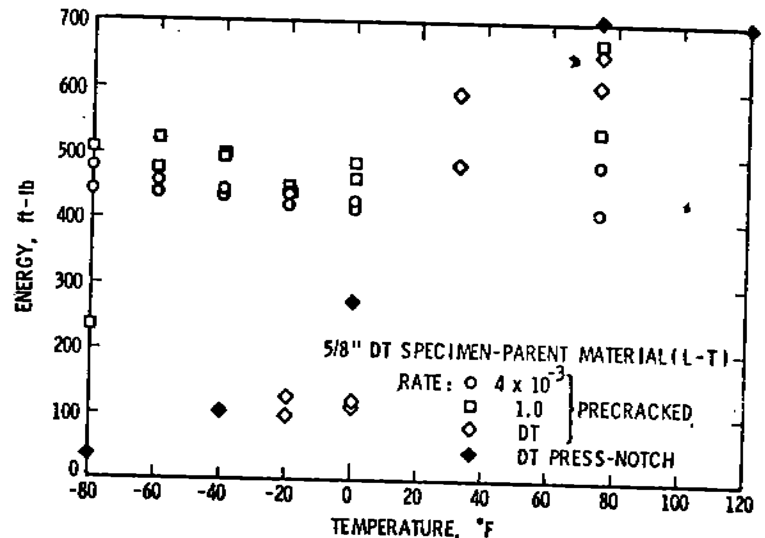

Figure 7. DT Energy, Heat No. 4 (CS)

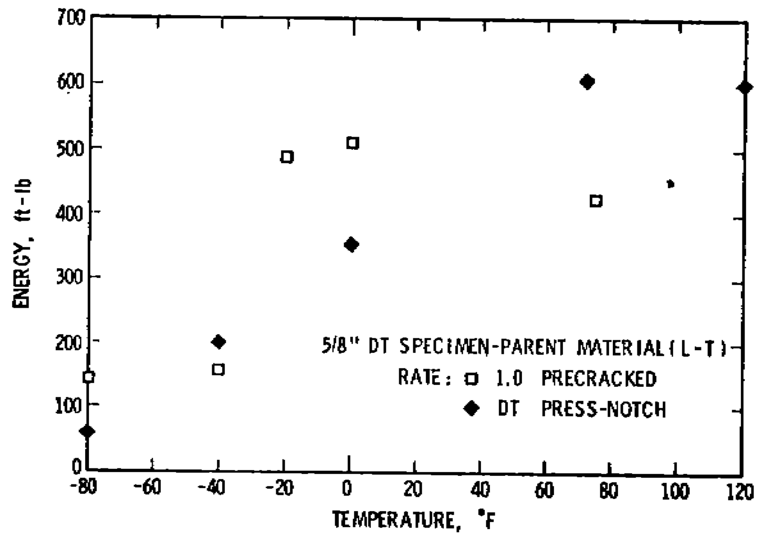

Figure 8. DT Energy, Heat No. 5 (A517-D)

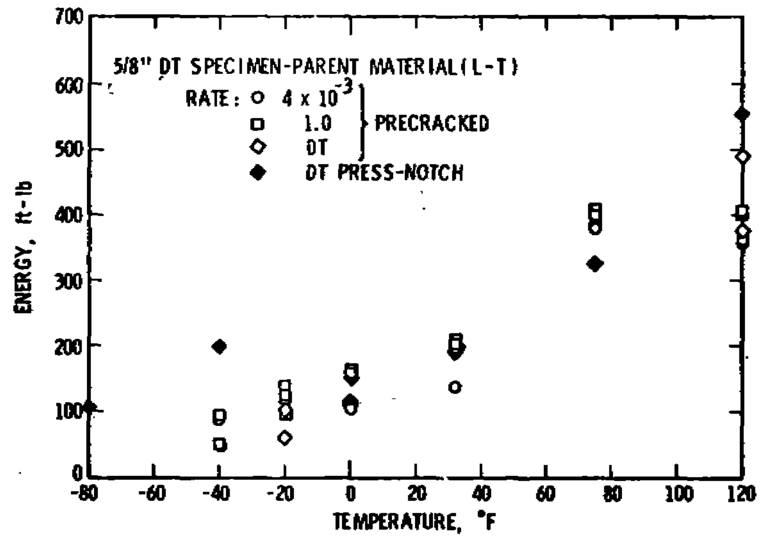

Figure 9. DT Energy, Heat No. 6 (A517-D)

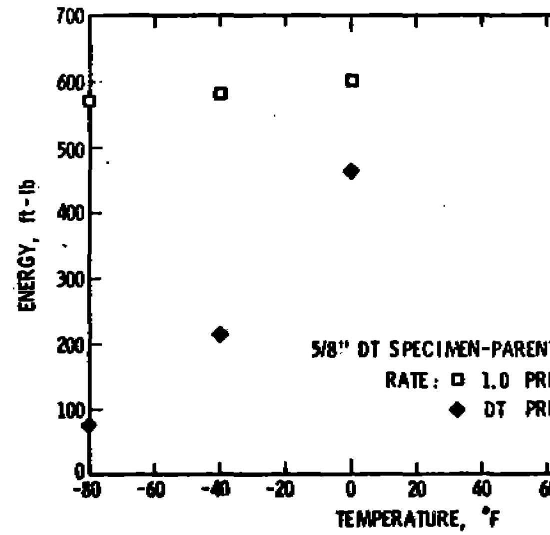

Figure 10. DT Energy, Heat No. 7

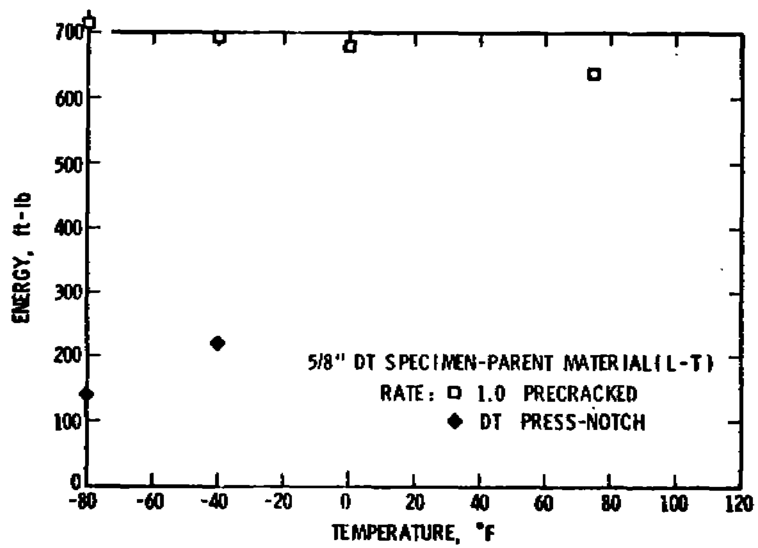

Figure 11. DT Energy, Heat No. 8 (A678-C)

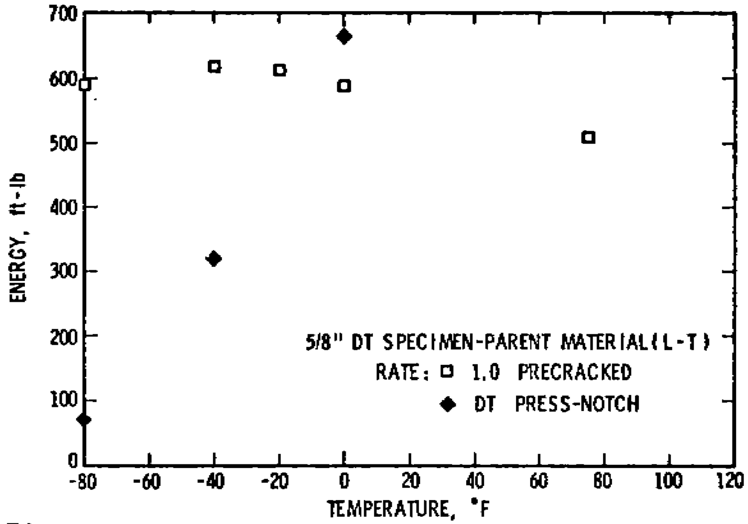

Figure 12. DT Energy, Heat No. 9 (A537-B)

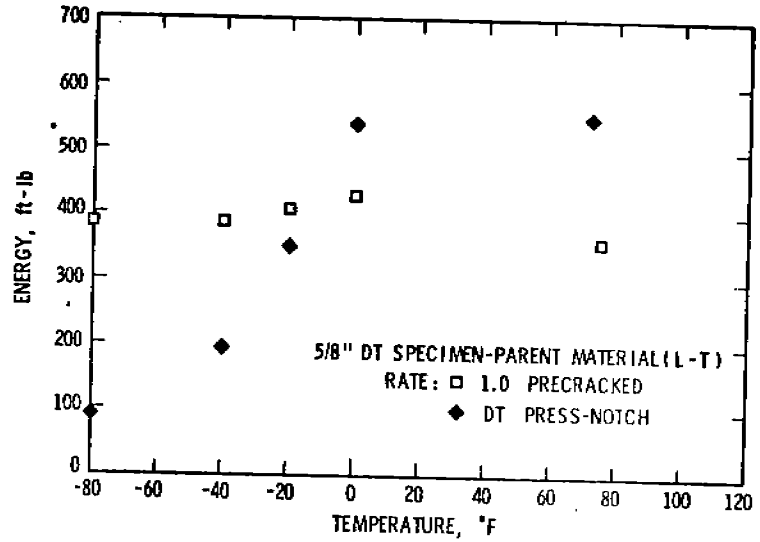

Figure 13. DT Energy, Heat No. 10 (A537-B)

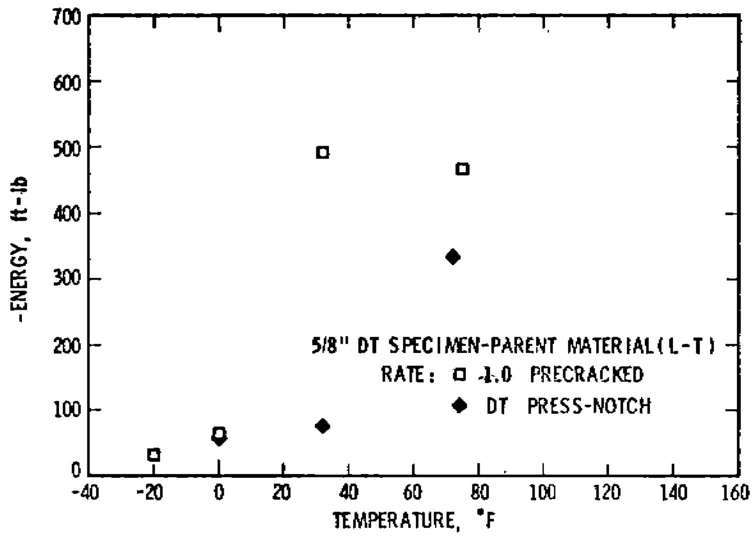

Figure 14. DT Energy, Heat No. 11 (ABS-B)

Despite the fact that it was not possible in every case to define both shelves in the test temperature range of -80°F to 160°F, not to mention data scatter (especially in the transition region), it is possible to establish approximate upper shelf values for the heats tested. These values are given in Table 10. One important fact emerges from these results. In examining the data for the A517, A678, and A537 steels where two heats of each were tested it is seen that substantial heat-to-heat variations in energy-of-fracture may be found. The energy-of-fracture is composed of both crack initiation and crack propagation components. The relative magnitude of these components varies with temperature, load rate, and notch condition, as well as material. Apparently, rather large variations in these energy components may be expected to be found among various heats of the same material.

In four of the heats (Heats 1, 3, 4, and 6) specimens were tested at various load rates to determine rate effects on precracked DT energy levels. Table 11 presents the transition temperature range and the upper shelf energy levels for these heats. Several observations can be made from the data presented. First, the transition temperature region shifts to the right with increased load rate, i.e., the mean transition temperature increases. This shift is very small in the "static" to "dynamic" regime, i.e., up to 1 in/sec head rate, but jumps dramatically from the "dynamic" to the "impact" load rate. Thus, transition temperatures, as measured by the conventional DT test, must be considered high for materials loaded at lesser rates. Second, there appears to be a tendency for the width of the transition temperature regime to narrow with increased load rate. The data are not complete enough, however, to assert this observation with confidence, and further test work would be necessary to validate it. Third, the upper shelf DT energy level itself apparently increases with load rate.

The above observations lead to an empirical representation of the energy-to-fracture W_f on the upper shelf as a product of two functions

$$W_f = f(T)g(\ln \dot{\varepsilon})$$

where both f and g are (approximately) linearly increasing functions of their respective arguments.

Figures 6, 7, and 9, on which the data for press-notch specimens are combined with the precracked specimen data, allow an evaluation to be made of notch tip condition. The general configuration of the three curves is similar but, at first, it appears that there are some differences. The data for the EH-32 steel displays similar behavior between the notched and precracked specimens over the entire temperature range. The A517 also shows similar behavior for the two notch tips except that

Table 9. 5/8" Dynamic Tear Test Results. Press Notch, L-T Orientation, Impact Loading (From SSC-276, Reference (3))

Heat No.	Material	Ft.-Lb. Energy Absorbed at Temperature (in °F)										
		-110	-80	-40	-20	0	32	75	100	120	160	200
2	AH-32					30		100	195	275	425	505
3	FH-32		35	90		265	665	660		640		
4	ABS-CS		35	105		275	745	705		700		
5	A517-D	100	60	200		405		610		605		
6	A517-D		105	200		155		325		555	585	
7	A678-C	45	75	215		465		785		765		
8	A678-C	35	140	220	950	1105		1040				
9	A537-B	35	70	320		665		790		885		
10	A537-D	45	90	195	350	540		550				
11	ABS-D					65	75	335	735	795	760	460

Table 10. Approximate Upper Shelf Energies for Precracked DT Specimens at Inter-Mediate Load Rate (Cross-Head Rate = 1 In/Sec)

Heat No.	Material	DT Energy, Ft-Lb
1	ABS-DS	550
2	AH-32	310
3	EH-32	500
4	ABS-CS	500
5	A517-D	500
6	A517-D	400
7	A678-C	650
8	A678-C	700
9	A537-B	600
10	A537-B	400
11	ABS-B	480

Table 11. Effect of Load Rate of and Upper Shelf DT Energ

Heat No.	Load Rate	Material	Transition Temperature Range, °F
1	static	ABS-DS	-80 to 50
1	dynamic	ABS-DS	-40 to 60
1	impact	ABS-DS	20 to 100
3	static	EH-32	? to -60
3	dynamic	EH-32	? to -60
3	impact	EH-32	-20 to 20
4	static	ABS-CS	< -80
4	dynamic	ABS-CS	? to -80
4	impact	ABS-CS	0 to 40
6	static	A517-D	20 to 60
6	dynamic	A517-D	0 to 70
6	impact	A517-D	0 to 80

Load Rate

Static = 4×10^{-3} in/sec
Dynamic = 1 in/sec
Impact = DT rate

the upper shelf energies are higher for the press notched specimen. This difference, on the order of 60-200 ft-lbs, indicates that, in the ductile region, large amounts of deformation takes place near the pressed notch before crack propagation begins. In the transition region, however, there is no difference between the two notches. This means that even though completely brittle conditions do not exist, the pressed notch is able to form a crack easily over at least part of the notch front and that this crack readily propagates in spite of the developing shear lips. It is also of interest to note that, unlike the EH and CS materials, the transition region in the A517 is not abrupt and extends over a large temperature range.

The CS material appears to show more signs of notch sensitivity, although this is not completely clear. The CS material displays higher upper shelf energies for the pressed notch, just as does the A517. If one takes the existing press notch data, then it appears that there is an effect of notch acuity in the transition region also. However, the energy recorded at 32°F is higher than the other upper shelf values at higher temperatures and is therefore suspect. At the lower end of the transition, the data indicate that the departure from exclusively brittle behavior begins 40°F earlier for the pressed notch specimen. It should be noted that there are no other data points in this temperature range. Hence, a press notch specimen could be completely brittle at -20° or even -10°F; this would cut the 40°F difference to 10° or 20°F, which is similar to the difference seen in many transition experiments. For example, for EH-32, at 0°F, the impact energies for the pressed notch and precracked specimens are the same. If these points are connected to the energies at the next lower temperature, then there is a difference of 20°F in the beginning of the transition region. If, however, one were to perform a pressed notch test at -20°F, then it would be possible to say whether or not there actually is a difference in the commencement of mixed brittle-ductile behavior. At present, there are not enough data to be able to say confidently there is a difference in the behavior of the two notch types.

If there is an effect of notch geometry, then it probably reflects a notch tip plasticity effect. For the CS plate, at 0°F, using the high rate values, the conventional plastic zone size estimate is

$$r_p = \frac{1}{2\pi} \left(\frac{K}{\sigma_y}\right)^2 = 0.035 \text{ inch.}$$

At the higher temperature of 75°F, the zone is

$$r_p = 0.437 \text{ inch}$$

and so the transition from plane strain to plane stress occurs in this regime. If the press notch is not sufficiently sharp, then it could cause the through thickness effects to occur slightly earlier than they would for the fatigue cracked specimen.

Unfortunately, there are no 0°F toughness data for either the EH-32 or the A517 to make the same comparison. Even at 75°F, we have only data for the latter, where

$$r_p = 0.276 \text{ inch.}$$

This would put the material in transition so one might expect to see some difference. However, the fracture mode in the high strength materials tends more toward cleavage under these conditions and so both the EH-32 and the A517 could cleave before the full extent of the through thickness effect is felt.

In summary, the energy-to-fracture W_f is higher for the press notch specimen than for the precracked specimen. The difference in DT energies is attributable to crack initiation, for the energy to propagate the crack to failure should be the same in both specimens. Since there is a significant difference in upper shelf energy, as reflected by the two kinds of notch conditions, it appears as though crack initiation is a significant, if not the dominant, portion of the total energy used to fracture a DT specimen on the upper shelf.

2. Instrumented Specimen Tests

A number of DT tests were conducted in which the specimen and load tup were instrumented in an effort to derive additional information from each test. In particular, all specimens from Heat No. 4 (ABS-CS)were instrumented, as were the room temperature specimens for all heats tested at the "dynamic" or intermediate head rate of 1.0 in/sec. In total, 32 specimens from Heat 4, and 2 specimens from all other heats tested were instrumented. In all cases the instrumented specimen was fitted with a crack opening displacement (COD) gage as described in Section III.C; in some cases a strain gage was also used on the specimen. Data readout consisted of time histories of load, displacement (or velocity), COD, and strain.

Before discussing the data analysis from the instrumented specimen tests, it is useful to review briefly several approaches to impact specimen data analysis which have been described in the recent literature. Each, of course, has certain advantages and disadvantages. As in most test procedures, increased data acquisition is obtained only through increased cost and complexity. This means that different procedures will have more or less utility for different users, depending upon the technical objectives.

From the standpoint of simplicity of use, certainly the first choice is to characterize fracture resistance of the DT specimen by measuring total energy-to-fracture, W_f , which is defined as the integral of force times the head displacement, taken over the displacement to failure, X_f . This method is analogous to the Charpy test which is also analyzed in terms of W_f , and is useful for comparing the relative fracture performance of various steels or as a screening or quality control test for heats of a given steel. It is simple, does not require the use of an instrumented specimen, and is inexpensive to conduct. Furthermore, the proposed SSC-244 criterion is written in terms of W_f as an acceptance criterion, viz., the material should exhibit a DT energy-to-fracture W_f of 250 ft-lbs (3000 in-lb) as measured with a 5/8" specimen having a 40 ksi static yield strength, tested at 75°F. (The W_f requirement increases with yield strength so as to insure a notch toughness of $K_{1d}/\sigma_{yd} = 0.9\sqrt{in}$.)

Despite the obvious advantages of W_f as a toughness criterion, it suffers several shortcomings, most of which stem from the fact that W_f lumps together the work done during fracture initiation with the energy which propagates the crack to failure. These two components of W_f are weighted quite differently depending upon the particular temperature and load rate test conditions. Thus, W_f can not be used to derive "true" measures of notch toughness (K_c or J_c) which are related to the energy required to initiate crack growth. This is a serious handicap in terms of ordinary strength and Q&T ship steels tested at 75°F, which are highly ductile and where much of W_f is consumed in propagating the crack. Moreover, when used in connection with the DT machine (an open loop test), both material and inertial effects are combined and reflected in W_f; inertial forces can be substantial and mask the true material behavior. Despite these disadvantages, W_f can be correlated with toughness for a given material, making it a useful parameter for the analysis of test data.

A second popular approach to interpreting DT test data is the nonlinear critical strain energy release rate, or J_{Cd}. This method is a generalization of the G_C derived for linearly elastic materials. J_C is proportional to the area under the force-displacement curve up to the point of crack initiation. The usefulness of J_{Cd} as a dynamic toughness measure is that it derives from basic fracture mechanics principles and applies to cases involving small-to-moderate crack tip plasticity. Also, from J_{Cd} one can derive an estimate on K_{Cd} under certain circumstances.

The major drawback to the use of J_{Cd} is the practical matter of defining the onset of crack propagation. For lack of a more satisfactory definition, crack initiation is usually associated with peak load. Recent research at the NRL reports that if fracture develops after general yield initiates, the dynamic fracture toughness can be computed using energy to maximum load (corrected for machine compliance) in conjunction with the J-integral approximate equation for a deeply notched beam in bending:

$$K_{Cd} = \sqrt{EJ_{Cd}} = \sqrt{\frac{2W_m E}{bB}} \tag{11}$$

where

$$W_m = \int_0^{x_m} P dx = \int_0^{t_m} PV dt = V_0 \int_0^{t_m} P dt \tag{12}$$

In these expressions E is Young's modulus, b the unbroken ligament length, B the specimen thickness, x_m and t_m the displacement and time associated with maximum load, respectively, and V_0 the average striker velocity associated with crack initiation. If fracture of the DT specimen develops prior to general yield, the maximum load P_m , together with the ASTM E 399 equation for K_{IC} under static loading, can be used to calculate dynamic fracture toughness if the E 399 rules apply and if the dynamic yield stress is used.

The limitations of J_{Cd} are twofold: first there is the difficulty in defining initiation, and second, the fact that J does not include inertial effects associated with dynamic deformation. In ductile materials such as ship steels at temperatures above the NDT, techniques such as heat tinting have been used to indicate initiation, but physical processes such as crack opening stretch lead to local unloading, which invalidates the basic assumptions behind J_C . Also, since the calculation of J is, in principle, a static calculation, there is no way to separate inertial forces from material behavior, so that J_{Cd} has limited meaning.

Another approach to DT data analysis that has been applied to a more limited extent is known as the equivalent energy method. This approach proposes to determine the fracture toughness, K_C , of a specimen which does not meet E 399 elastic-plastic fracture requirements (e.g., the DT specimen) by the plane strain value K_{IC} and a "scaling factor":

$$K_C = \sqrt{\frac{\text{volumetric energy ratio}}{\text{ratio of specimen scale}}}\; K_{1C} \tag{13}$$

Here, the volumetric energy ratio is the ratio of the fracture energy to maximum load for two geometrically similar specimens of the same material at the same temperature, the thicker of which gives a valid K_{1C} .

This approach suffers from the same limitations as does J_C regarding the definition of initiation; and it, too, ignores inertial effects. Moreover, it requires a control DT specimen of a different size to use it, ignoring the fact that these two specimens will generally have different crack tip plastic strain distributions.

A final approach to data interpretation which should be mentioned is the relation between K_C and the critical crack opening displacement (COD_C) or the critical crack tip opening displacement ($CTOD_C$). This approach can be discussed in the following way. In a DT test the tup motion loads the specimen with a known time-dependent force P(t) relationship, which in turn produces a COD and a CTOD which are functions of the material behavior and inertial effects. The dynamic K_C value, K_{Cd} can be calculated by an approach similar to the NRL analysis based on a Timoshenko beam model. The specimen is idealized as two elastic members connected by an elastic spring, and the analysis calculates K(t) output as a function of P(t) input. The details of the analysis, yet unpublished, require the solution of an integral equation containing the normal beam functions, and is quite involved. The method is quite sensitive to a number of factors which are difficult to obtain from the impact system. Even if the calculation is accepted as correct, the problem of establishing the critical value of the dynamic K, persists. It is worth noting that according to NRL, the use of a static analysis procedure will generally lead to erroneous K_{Cd} values.

Rather than using P(t) to determine toughness as a function of time, it is natural to attempt to utilize the crack opening displacement (COD) as a direct measure of material toughness. At first glance, this method is attractive as it proposes to use a measured quantity to characterize toughness.

By making certain assumptions regarding the similarity of specimen displacement (not specimen strain) behavior in the static and dynamic modes, one can calculate the crack tip opening displacement (CTOD) as a function of time. However, in order to apply this concept, one must experimentally determine a critical CTOD, which is a very difficult task. Alternately, the CTOD can be related to the stress intensity factor in the manner promoted by British and Japanese scientists in recent years. Unfortunately, this largely negates the advantage of the dynamically measured COD by requiring the introduction of the crack tip strain field. As presently used for static analysis, the CTOD is obtained from the Dugdale model and this model is not even representative of the static plastic zone in ship steels, let alone the dynamic zone. The difficulties with using CTOD(t) are twofold, then. First, the kinematic model is approximate as it assumes rigid body motion. Second, the lack of dynamically determined critical values of CTOD constitutes a formidable barrier. As a longer term research tool, this method is attractive. However, in the short run, the method is beset with so many approximations as to possess very limited meaning in evaluating the DT test results.

The primary objective in analyzing the DT data in the present investigation was to relate yield load, P_y, energy-to-failure, W_f, and fracture toughness K_c to loading rate and temperature. The quantities needed to calculate these parameters were determined from data traces recorded during the tests. All of the DT tests conducted on Heat No. 4 (ABS-CS) specimens, as well as the room temperature tests at the dynamic (intermediate) rate on the remaining heats, and one impact test each on Heats 6 (A517-D) and 10 (A537-B) were instrumented with COD gages, and in some cases transient strain records were obtained from a strain gage mounted on the specimen as explained in Section III.C. Data traces for the instrumented tests consisted of time histories of driving point load, velocity, COD, and strain, where applicable. All other tests at the impact rate on the DT machine were conducted so as to record total energy-to-failure W_f only. For the remaining tests at static and dynamic load rates, the time-dependent load and head displacement were recorded. The transient data recorded from tests at all three loading rates were digitized and placed on magnetic tape casettes for cross-plotting and data reduction on a Hewlett-Packard HP-9830 computer.

Data reduction techniques differed somewhat for the impact test results as compared with the data from the static and dynamic tests. In the case of the static and dynamic tests, the yield load P_y was determined by cross-plotting load P against (head) displacement x, then locating the load at which the relationship became nonlinear. The maximum load P_m was also determined from these plots, and the displacement at maximum load,

x_m, was then determined from the P-x plot. The energy to maximum load, W_m, and the total energy to failure, W_f, were calculated by numerical integration of the P-x record to the appropriate displacement.

The data reduction procedures for the instrumented impact tests were somewhat more involved because of the high harmonic content in the records stemming from specimen dynamics. The load-time record first was smoothed by fitting a curve through the mean of the oscillations describing the dynamic, inelastic response. Then, using the load-displacement elastic compliance determined from the dynamic (intermediate load rate) test results, a straight load-time line was drawn from zero load to its intersection with the smoothed curve mentioned above. This procedure assumes that the specimen loads elastically and that the stiffness during elastic loading is the same for both dynamic and impact loading. The load corresponding to the intersection of the assumed elastic loading line with the smoothed inelastic loading curve was defined as P_y, the yield load for the impact case. The smoothed inelastic curve was also used to pick off the maximum load P_m. The energy-to-maximum load, W_m, was calculated by integrating along the assumed elastic and inelastic loading path to P_m. This procedure obviously requires some judgement, and the results must be regarded as estimates only. The energy-to-failure, W_f, was read directly off the DT machine.

These calculations for the tests at all three load rates were then used to determine a fracture toughness parameter. Equation (11) was used to calculate a dynamic fracture toughness parameter, K_{Cd}, from the energy-to-maximum load, W_m, and the geometric parameters of the specimen.

Figures 15-17 show load-deflection curves for Heat 4 (ABS-CS); these curves are typical of those found for all heats. Figures 15 and 16 indicate how the response varies with temperature at two loading rates, and Figure 17 shows the response at static, dynamic, and impact rates all at room temperature. At static and dynamic loading rates, decreasing temperature is associated with the more pronounced development of a lower yield point, and with an increase in maximum load. In all cases with the exception of the A517-D, significant yield preceded fracture at room temperature.

An example to show how the impact response of an instrumented DT specimen varies with temperature either side of the transition regions is given in Figures 18-23. Figures 18-20 show the detailed time histories of tup load, tup velocity, COD, and strain near the crack tip on a specimen from Heat No. 4 (ABS-CS), impact tested at room temperature. Figure 18 reveals the harmonic content of the driving point load. The record shows a high fundamental mode content with a frequency of about 7 kHz, although the third mode is also present. The velocity

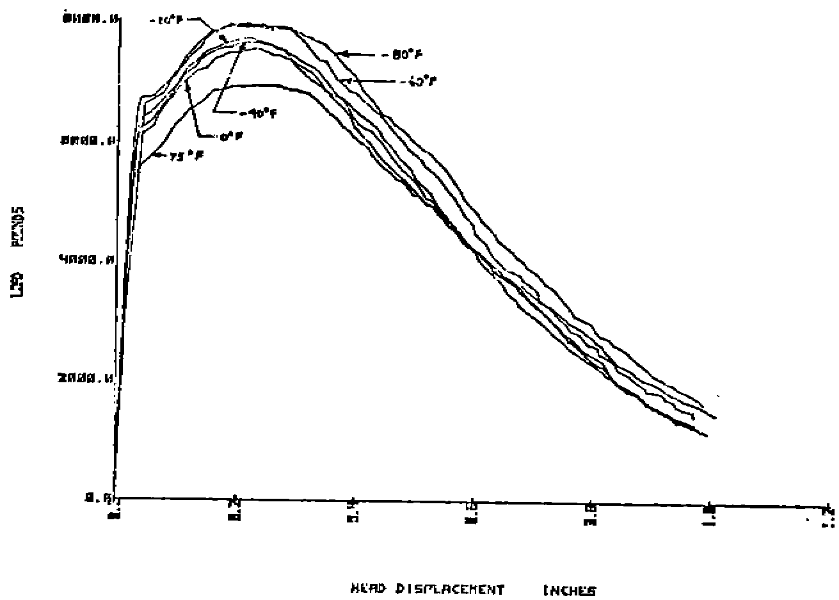

Figure 15. DT Load-Displacement Heat No. 4 (ABS-CS) 4 x 10^{-3} In/Sec Load Rate

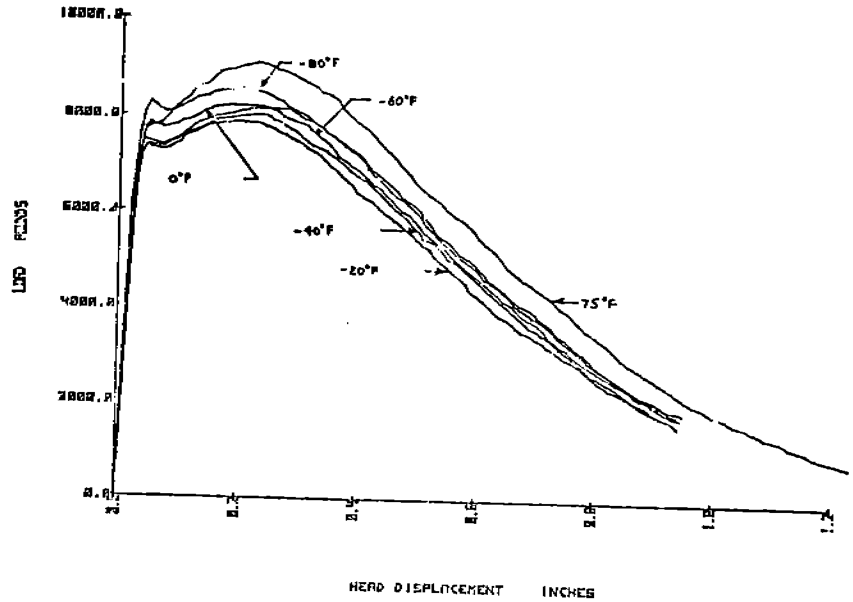

Figure 16. DT Load-Displacement Heat No. 4 (ABS-CS) 1 In/Sec Load Rate

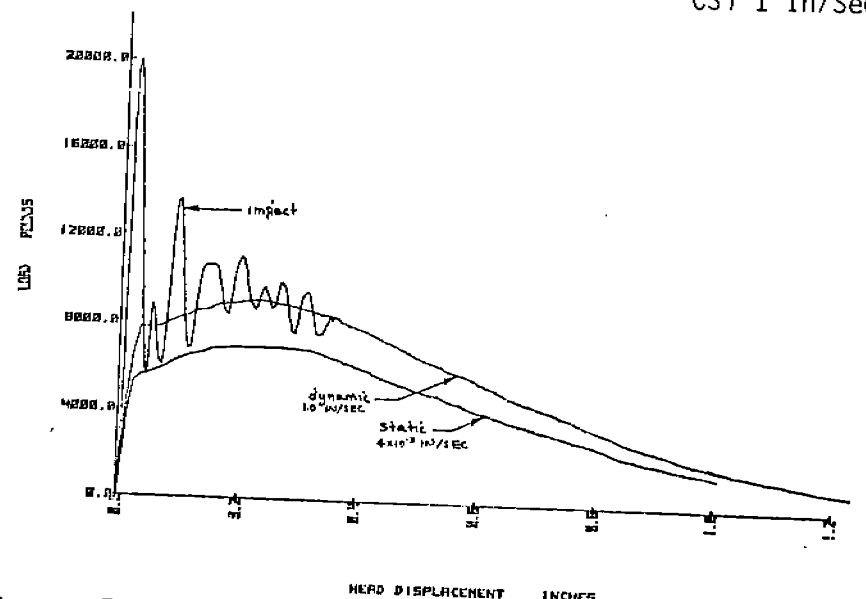

Figure 17. DT Load-Displacement Heat No. 4 (ABS-CS) $75^{o}F$

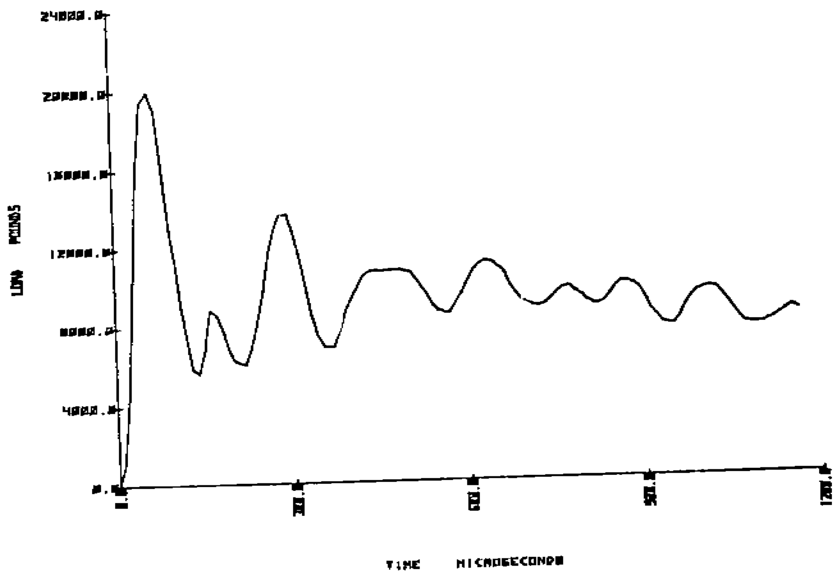

Figure 18. DT Impact Load-Time History Heat No. 4, 75°F

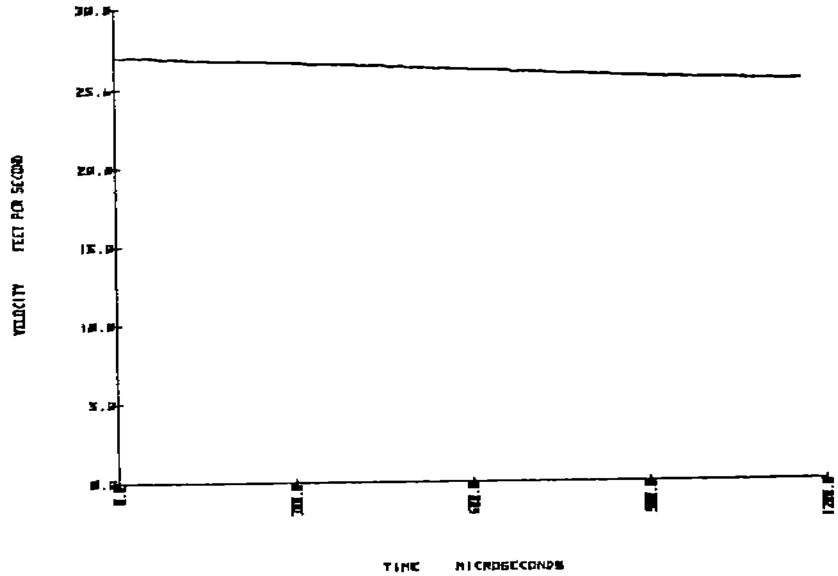

Figure 19. DT Impact Velocity-Time History Heat No. 4, 75°F

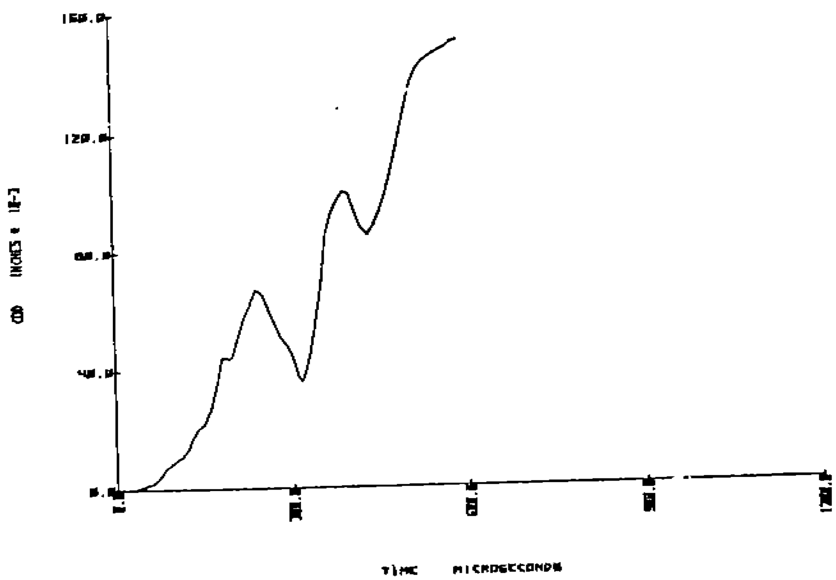

Figure 20. DT Impact COD-Time History Heat No. 4, 75°F

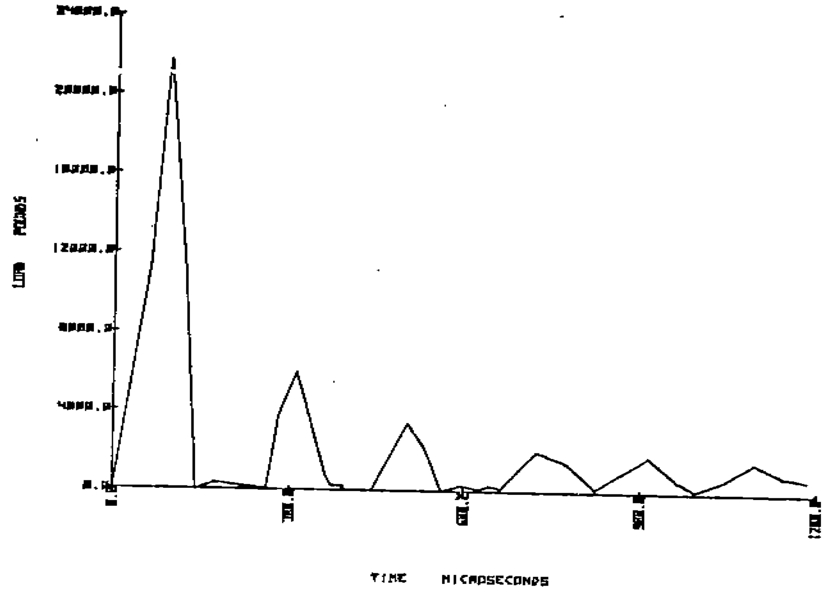

Figure 21. DT Impact Load-Time History Heat No. 4, $-20^{0}F$

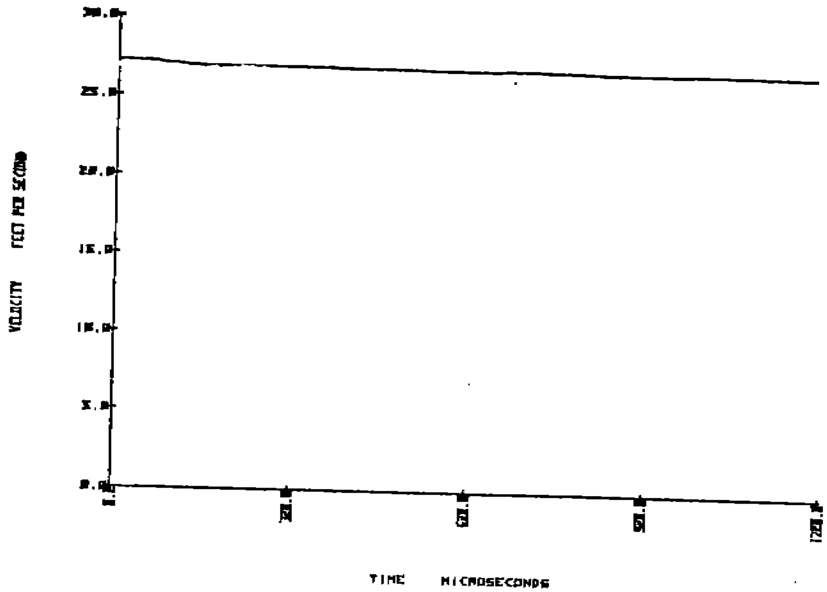

Figure 22. DT Impact Velocity-Time History Heat No. 4, $-20^{0}F$

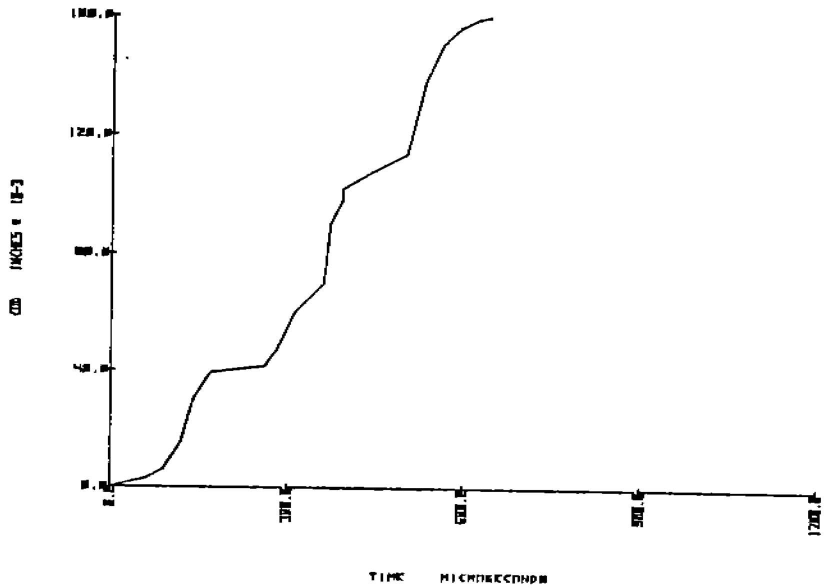

Figure 23. DT Impact COD-Time History Heat No. 4, $-20^{0}F$

of the loading tup is seen to decrease linearly and vary slightly with time during the impact event. The impact velocity can, for practical purposes, be considered equal to the initial impact velocity over the time interval where the specimen behaves elastically. Figure 20 indicates that the COD is composed of a linearly increasing component, superimposed upon which is harmonic motion of about the same frequency as the loading tup motion. A time delay of about 85 μsec is found between the tup input and the COD response.

Figures 21-23 show the time histories of the loading tup, tup velocity, and COD for a specimen from Heat 4 as above, but tested at -20°F, below the transition temperature (see Figure 7). The records are not as smooth as the preceding records because a coarser digitizing spacing was used. Nevertheless, the major features of the transient records are present. Figure 21 indicates that the specimen broke shortly after the initial dynamic spike, and the load tup continued to ring against the specimen. Figure 23 supports this conclusion by indicating that the COD increased continuously with time, with no oscillation as in the case of the specimen tested above the transition temperature.

Tables 12-22 contain, for each of the eleven heats, a complete summary of the data from the DT tests. In order to illustrate the trends suggested by the data, Figures 24-32 have been prepared to demonstrate the rate and temperature dependence of the DT test parameters for Heats No. 4 (ABS-CS) and 6 (A517-D). These figures indicate how yield load P_y, energy-to-failure W_f, and fracture toughness K_c are affected by load rate and temperature. Figures 28 and 29, which show the relationship between W_f and T for Heats 4 and 6 are repeats of Figures 7 and 9, but are included here again for convenience in interpreting this group of figures.

In this program, the CS material was the most extensively tested material, and Figures 27, 28, 30, and 31 present some interesting results. The usual tendency is for the temperature vs energy-to-fracture curve to be shifted to the right as the load rate is increased. Figures 27 and 28 illustrate that this effect is not very large for the CS plate until impact rates are recorded. Figure 27 shows that at slow rates, there is little effect of temperature, while at impact rates, the low temperatures take little energy to failure while the higher temperature tests absorb a considerable amount of energy. Figure 28 also illustrates the general lack of temperature effect except at the impact rate.

This performance can be contrasted with the dynamic toughness, which is more representative of the fracture initiation properties of a material. Figure 30 shows that regardless of temperature, the dynamic toughness of CS plate measured by impact testing is very low. In fact, as shown by Figure 31, the temperature transition shift from the quasi-static is very

Table 12. 5/8" Dynamic Tear Test Summary, Heat No. 1 (ABS-DS)

Temp. °F	Head Rate (in/sec)	Yield Load P_y (lb)	Max. Load P_m (lb)	Defl. At Max. Load X_m (in)	Energy To Max. Load W_m (ft-lb)	Energy To Failure W_f (ft-lb)	"Fracture Toughness" K_c (ksi$\sqrt{in}$)
	4×10^{-3}	6391/6130	9132/8758	.134/.122	82/70	86/74	301/278
-80	1.0	8434/5608	8434/5645	.030/.021	10.3/4.4	13.4/8	107/69.6
	DT*	-	-	-	-	-	-
	4×10^{-3}	4989/6000	9029/8986	.266/.237	169/146	311/148	432/401
-40	1.0	6262/8751/6884	8144/10061/9657	.084/.162/.190	46/116/128	80/468/137	225/358/376
	DT*	-		-	-	-	-
	4×10^{-3}	4278/4676	9016/8902	.281/.248	177/153	402/198	442/411
-20	1.0	7755/7015	9890/8965	.233/.158	157/97	183/167	416/327
	DT*	-	-	-	-	-	-
	4×10^{-3}	4930/3587	9501/9284	.299/.199	199/132	397/428	468/381
0	1.0	6421/5620	9644/9188	.284/.163	196/102	409/206	465/335
	DT*	-	-	-	-	15/20	-
	4×10^{-3}	5478/5517	8981/8353	.283/.266	178/158	602/559	443/417
32	1.0	6706/4220	9705/9517	.286/.289	197/197	422/518	466/466
	DT*	-	-	-	-	85/555	-
	4×10^{-3}	5515/5839	8775/9187	.341/.225	212/141	651/622	483/394
75	1.0	5181/5142	8000/7668	.291/.350	168/156	538/511	
	DT*	-	-	-	-	275/260	-
	4×10^{-3}	-	-	-	-	-	-
120	1.0	-	-	-	-	-	-
	DT*	-	-	-	-	525/530	-
	4×10^{-3}	-	-	-	-	-	-
160	1.0	-	-	-	-	-	-
	DT*	-	-	-	-	800/880	-

*Approx. 315 in/sec, initial impact.

Table 13. 5/8" Dynamic Tear Test Summary, Heat No. 2 (ABS AH-32)

Temp. °F	Head Rate (in/sec)	Yield Load P_y (lb)	Max. Load P_m (lb)	Defl. At Max. Load X_m (in)	Energy To Max. Load W_m (ft-lb)	Energy To Failure W_f (ft-lb)	"Fracture Toughness" K_c (ksi $\sqrt{in}$)
0	4×10^{-3}	–	–	–	–	–	–
	1.0	9223	9236	.033	12.7	35	118
	DT*	–	–	–	–	–	–
32	4×10^{-3}	–	–	–	–	–	–
	1.0	8489	11193	.108	82	148	301
	DT*	–	–	–	–	–	–
75	4×10^{-3}	–	–	–	–	–	–
	1.0	7965	10400	.119	64	312	–
	DT*	–	–	–	–	–	
120	4×10^{-3}	–	–	–	–	–	–
	1.0	8288	10129	.102	70	311	278
	DT*	–	–	–	–	–	–

*Approx. 315 in/sec, initial impact.

Table 14. 5/8" Dynamic Tear Test Summary, Heat No. 3 (ABS EH-32)

Temp. ^oF	Head Rate (in/sec)	Yield Load P_y (lb)	Max Load P_m (lb)	Defl. At Max. Load X_m (in)	Energy To Max. Load W_m (ft-lb)	Energy To Failure W_f (ft-lb)	"Fracture Toughness" K_c (ksi $\sqrt{in}$)
-80	4×10^{-3}	7579/7814	9328/9248	.151/.185	99/127	225/411	330/374
	1.0	8524/8655	10638/10176	.133/.129	102/94.4	265/440	335/323
	DT*	-	-	-	-	-	-
-40	4×10^{-3}	7205/6176	9345/9113	.169/.145	111/92	422/398	350/318
	1.0	6856/7493	10258/10342	.155/.162	111/122	507/488	350/367
	DT*	-	-	-	-	-	-
-20	4×10^{-3}	6570/7133	9217/9345	.151/.171	97/113	414/439	327/353
	1.0	8620/8731	10397/9900	.155/.151	115/110	505/483	356/348
	DT*	-	-	-	-	65/75	-
0	4×10^{-3}	5974/6593	9176/9049	.172/.168	111/105	460/442	350/340
	1.0	7569/6675	9781/9719	.211/.182	152/123	488/484	409/368
	DT*	-	-	-	-	230/240	-
32	4×10^{-3}	-	-	-	-	-	-
	1.0	-	-	-	-	-	-
	DT*	-	-	-	-	530/600	-
75	4×10^{-3}	5008/4068	8596/7223	.170/.165	102/84	435/338	335/304
	1.0	5275/6667	7706/7856	.193/.201	109/115	405/398	347/356
	DT*	-	-	-	-	540/570	-
120	4×10^{-3}	-	-	-	-	-	-
	1.0	-	-	-	-	-	-
	DT*	-	-	-	-	515/530	-

*Approx. 315 in/sec, initial impact.

Table 15. 5/8" Dynamic Tear Test Summary, Heat No. 4 (ABS CS)

Temp. ^{o}F	Head Rate (in/sec)	Yield Load P_y (lb)	Max. Load P_m (lb)	Defl. At Max. Load X_m (in)	Energy To Max. Load W_m (ft-lb)	Energy To Failure W_f (ft-lb)	"Fracture Toughness" K_c (ksi$\sqrt{in}$)
	4×10^{-3}	6275/6629	7891/7962	.215/.212	123/119	442/478	368/362
-80	1.0	6197/6619	8566/7980	.213/.042	137/16.7	507/234	389/136
	DT*	-	-	-	-	-	-
	4×10^{-3}	5469/5358	7663/7918	.203/.227	112/132	440/458	352/381
-60	1.0	6917/6996	8226/8651	.178/.199	107/124	525/477	344/370
	DT*	-	-	-	-	-	-
	4×10^{-3}	5895/6052	7625/7911	.239/.227	133/127	445/436	382/374
-40	1.0	5784/7231	8038/8211	.221/.230	132/139	495/498	381/391
	DT	-	-	-	-	-	-
	4×10^{-3}	5378/6282	7694/7711	.220/.204	122/115	421/439	367/356
-20	1.0	6753/6000	7889/7900	.196/.207	114/118	442/450	354/361
	DT*	3210/2775	3210/2775	.015/.013	2.0/1.5	96/126	47.0/40.7
	4×10^{-3}	6072/5076	7516/7433	.224/.258	121/140	417/429	365/393
0	1.0	6465/6701	7751/8170	.237/.225	134/134	462/487	385/385
	DT*	2880/2672	2880/2672	.013/.012	1.5/1.3	122/112	40.7/37.9
	4×10^{-3}	-	-	-	-	-	-
32	1.0	-	-	-	-	-	-
	DT*	10529/9386	10643/9386	.040/.035	17.6/13.7	593/485	139/123
	4×10^{-3}	4548/5265	6992/6951	.205/.223	107/96	486/412	343/325
75	1.0	6295/5784	9111/9039	.225/.234	156/172	538/669	415/435
	DT*	10298/9000	10298/9714	.033/.031	14.1/12.5	605/655	125/117

*Approx. 315 in/sec, initial impact.

Table 16. 5/8" Dynamic Tear Test Summary, Heat No. 5 (ASTM A517-D)

Temp. °F	Head Rate (in/sec)	Yield Load P_y (lb)	Max. Load P_m (lb)	Defl. At Max. Load X_m (in)	Energy To Max. Load W_m (ft-lb)	Energy To Failure W_f (ft-lb)	"Fracture Toughness" K_c (ksi$\sqrt{in}$)
-80	4×10^{-3}	-					
	1.0	11170	12367	.036	19.3	143	146
	DT*	-	-	-	-	-	-
-40	4×10^{-3}	-	-	-	-	-	-
	1.0	12183	14364	.045	28.1	156	176
	DT*	-	-	-	-	-	-
-20	4×10^{-3}	-	-	-	-	-	-
	1.0	14474	17455	.082	76.2	488	290
	DT*	-	-	-	-	-	-
0	4×10^{-3}	-	-	-	-	-	-
	1.0	12000	17333	.083	78.8	510	295
	DT*	-	-	-	-	-	-
75	4×10^{-3}	-	-	-	-	-	-
	1.0	9924	14542	.079	73	425	284
	DT*	-	-	-	-	-	-

*Approx. 315 in/sec, initial impact.

Table 17. 5/8" Dynamic Tear Test Summary, Heat No. 6 (ASTM A517-D)

Temp. °F	Head Rate (in/sec)	Yield Load P_y (lb)	Max. Load P_m (lb)	Defl. At Max. Load X_m (in)	Energy To Max. Load W_m (ft-lb)	Energy To Failure W_f (ft-lb)	"Fracture Toughness" K_c (ksi $\sqrt{in}$)
-40	4×10^{-3}	11074/8739	11091/8758	.031/.024	14.8/7.7	87/49	128/92.1
	1.0	5807/6930	9556/7831	.041/.022	20.2/6.8	94/49	149/86.6
	DT*	-	-	-	-	-	-
-20	4×10^{-3}	13262/9739	13932/9768	.043/.029	26.3/10.9	100/71	170/110
	1.0	9904/6646	10535/7753	.050/.041	27.0/17.1	118/96	173/137
		9511/7415	11118/9521	.043/.045	23.0/22.6	123/140	159/158
	DT*	-	-	-	-	60/100	-
0	4×10^{-3}	9827/12113	9827/12923	.032/.042	12.9/21.9	106/105	119/155
	1.0	7339/11763	9345/11751	.059/.039	32.7/19.3	157/159	190/146
	DT*	-	-	-	-	110/115	-
32	4×10^{-3}	10505/13309	13415/14083	.043/.047	23.9/27.6	197/137	162/174
	1.0	13092/9502	13117/12160	.038/.035	20.4/18.7	212/202	150/144
	DT*	-	-	-	-	190/220	-
75	4×10^{-3}	14,700/13225	15792/15386	.062/.061	43.8/45.1	380/385	220/223
	1.0	12478/12489	14348/13526	.096/.072	78/52	399/406	293/240
	DT*	13,472	13,472	.050	28.1	335	176
120	4×10^{-3}	9674/11739	14226/14400	.072/.068	57.3/53.5	357/361	251/243
	1.0	10793/12207	15940/15617	.059/.061	44.2/48.8	407/404	221/232
	DT*	-	-	-	-	375/490	-
160	4×10^{-3}	-	-	-	-	-	-
	1.0	-	-	-	-	-	-
	DT*	-	-	-	-	380/470	-

*Approx. 315 in/sec, initial impact.

Table 18. 5/8" Dynamic Tear Test Summary, Heat No. 7 (ASTM A678-C)

Temp. ^{o}F	Head Rate (in/sec)	Yield Load P_y (lb)	Max. Load P_m (lb)	Defl. At Max. Load X_m (in)	Energy To Max. Load W_m (ft-lb)	Energy To Failure W_f (ft-lb)	"Fracture Toughness" K_c (ksi $\sqrt{in}$)
-80	4×10^{-3}	-	-	-	-	-	-
	1.0	7140	13817	.114	108	571	345
	DT*	-	-	-	-	-	-
-40	4×10^{-3}	-	-	-	-	-	-
	1.0	9827	13782	.131	125	584	371
	DT*	-	-	-	-	-	-
0	4×10^{-3}	-	-	-	-	-	-
	1.0	7755	13521	.150	141	603	394
	DT*	-	-	-	-	-	-
75	4×10^{-3}	-	-	-	-	-	-
	1.0	8533	11813	.186	150	656	407
	DT*	-	-	-	-	-	-

*Approx. 315 in/sec, initial impact.

Table 19. 5/8" Dynamic Tear Test Summary, Heat No. 8 (ASTM A678-C)

Temp. °F	Head Rate (in/sec)	Yield Load P_y (lb)	Max. Load P_m (lb)	Defl. At Max. Load X_m (in)	Energy To Max. Load W_m (ft-lb)	Energy To Failure W_f (ft-lb)	"Fracture Toughness" K_c (ksi $\sqrt{in}$)
-80	4×10^{-3}	–	–	–	–	–	–
	1.0	11419	14647	.155	154	704	412
	DT*	–	–	–	–	–	–
-40	4×10^{-3}	–	–	–	–	–	–
	1.0	12180	14625	.160	160	694	420
	DT*	–	–	–	–	–	–
0	4×10^{-3}	–	–	–	–	–	–
	1.0	9365	12910	.172	157	680	416
	DT*	–	–	–	–	–	–
75	4×10^{-3}	–	–	–	–	–	–
	1.0	6911	11156	.189	148	638	404
	DT*	–	–	–	–	–	–

*Approx. 315 in/sec, initial impact.

Table 20. 5/8" Dynamic Tear Test Summary, Heat No. 9 (ASTM A537-B)

Temp. °F	Head Rate (in/sec)	Yield Load P_y (lb)	Max. Load P_m (lb)	Defl. At Max. Load X_m (in)	Energy To Max. Load W_m (ft-lb)	Energy To Failure W_f (ft-lb)	"Fracture Toughness" K_c (ksi$\sqrt{in}$)
-80	4×10^{-3}	–					
	1.0	5956	11977	.156	131	590	380
	DT*	–	–	–	–	–	–
-40	4×10^{-3}	–					
	1.0	9817	11960	.171	144	620	398
	DT*	–	–	–	–	–	–
-20	4×10^{-3}	–	–	–	–	–	–
	1.0	7460	11316	.164	133	613	383
	DT*	–	–	–	–	–	–
0	4×10^{-3}	–	–	–	–	–	–
	1.0	8246	10718	.181	138	588	390
	DT*	–	–	–	–	–	–
75	4×10^{-3}	–	–	–	–	–	–
	1.0	6996	8794	.170	105	510	340
	DT*	–	–	–	–	–	–

*Approx. 315 in/sec, initial impact.

Table 21. 5/8" Dynamic Tear Test Summary, Heat No. 10 (ASTM A537-8)

Temp. °F	Head Rate (in/sec)	Yield Load P_y (lb)	Max. Load P_m (lb)	Defl. At Max. Load X_m (in)	Energy To Max. Load W_m (ft-lb)	Energy To Failure W_f (ft-lb)	"Fracture Toughness" K_c (ksi $\sqrt{in}$)
-80	40×10^{-3}	–	–	–	–	–	–
	1.0	11616	13086	.059	40.5	385	211
	DT*	–	–	–	–	–	–
-40	4×10^{-3}	–	–	–	–	–	–
	1.0	8742	12205	.095	73.5	387	285
	DT*	–	–	–	–	–	–
-20	4×10^{-3}	–	–	–	–	–	–
	1.0	9520	12078	.102	83.7	407	304
	DT*	–	–	–	–	–	–
0	4×10^{-3}	–	–	–	–	–	–
	1.0	9331	11885	.104	83.5	428	303
	DT*	–	–	–	–	–	–
75	4×10^{-3}	–	–	–	–	–	–
	1.0	6174	10658	.104	74.8	358†	287
	DT*	12167	12167	.043	21.7	363	155

*Approx. 315 in/sec, initial impact.

†A specimen from Heat No. 10 was inadvertently run at 4×10^{-3} in/sec at 75°F and registered 199 ft-lbs.

Table 22. 5/8" Dynamic Tear Test Summary, Heat No. 11 (ABS B)

Temp. ^oF	Head Rate (in/sec)	Yield Load P_y (lb)	Max. Load P_m (lb)	Defl. At Max. Load X_m (in)	Energy To Max. Load W_m (ft-lb)	Energy To Failure W_f (ft-lb)	"Fracture Toughness" K_c (ksi $\sqrt{in}$)
-20	4×10^{-3}	-	-	-	-	-	-
	1.0	6688	7760	.032	10.6	32	108
	DT*	-	-	-	-	-	-
0	4×10^{-3}	-	-	-	-	-	-
	1.0	5754	7451	.030	10.1	64	106
	DT*	-	-	-	-	-	-
32	4×10^{-3}	-	-	-	-	-	-
	1.0	5902	9106	.209	137	491	389
	DT*	-	-	-	-	-	-
75	4×10^{-3}	-	-	-	-	-	-
	1.0	5827	7334	.284	150	466	407
	DT*	-	-	-	-	-	-

*Approx. 315 in/sec, initial impact.

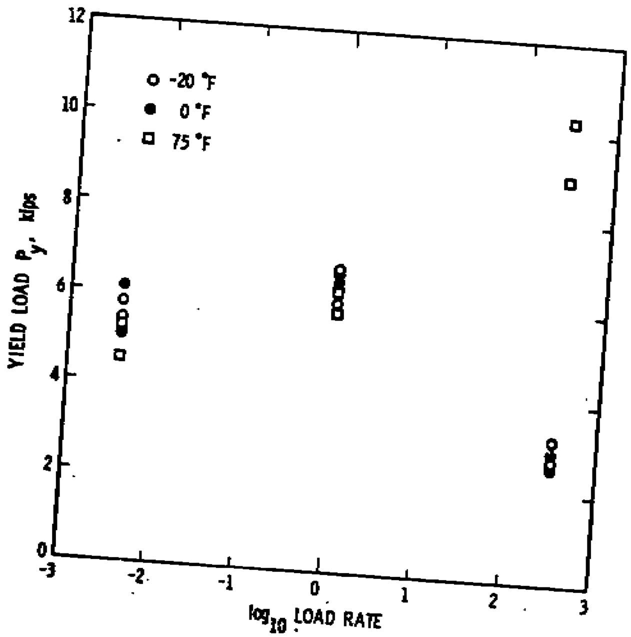

Figure 24. Rate Dependence of DT Yield Load, Heat No. 4 (ABS-CS)

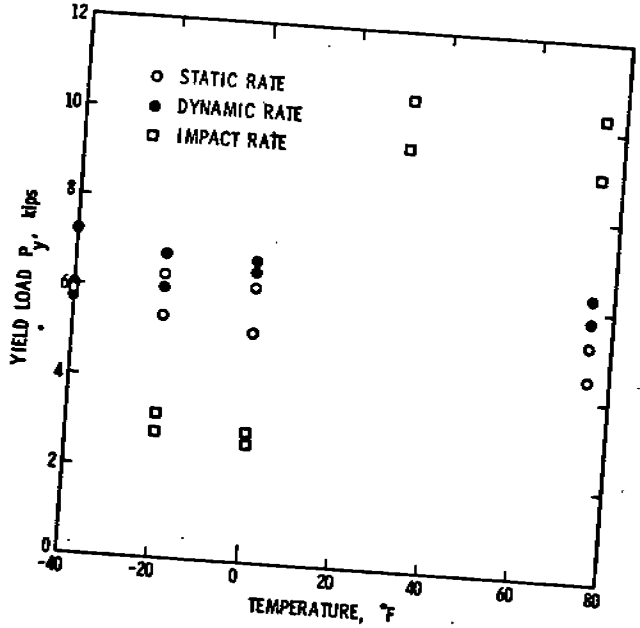

Figure 25. Temperature Dependence of DT Yield Load, Heat No. 4 (ABS-CS)

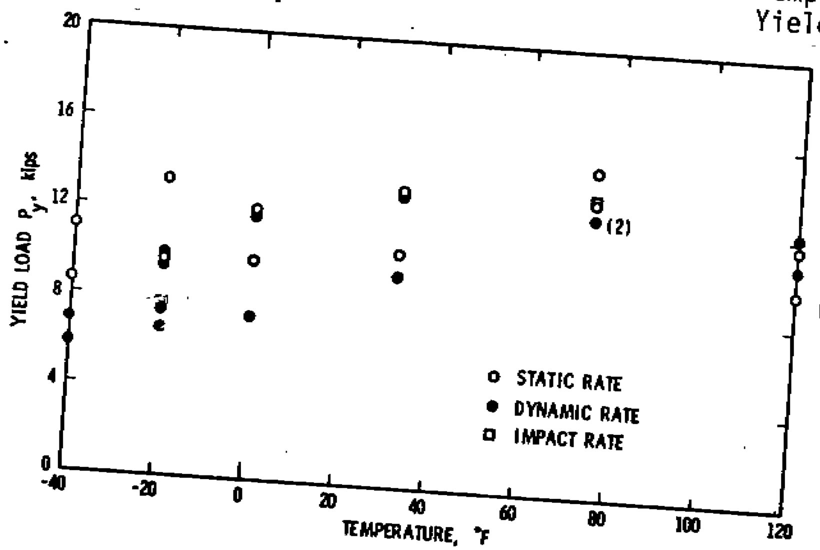

Figure 26. Temperature Dependence of DT Yield Load, Heat No. 6 (A517-D)

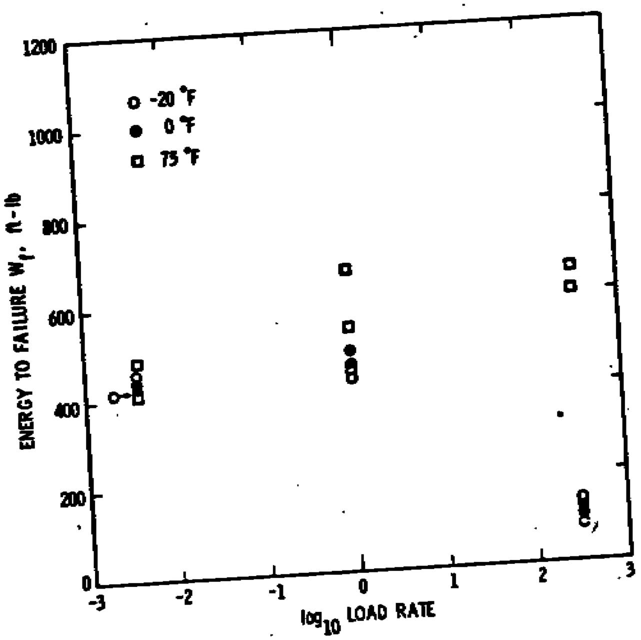

Figure 27. Rate Dependence of DT Energy-to-Failure W_f, Heat No. 4 (ABS-CS)

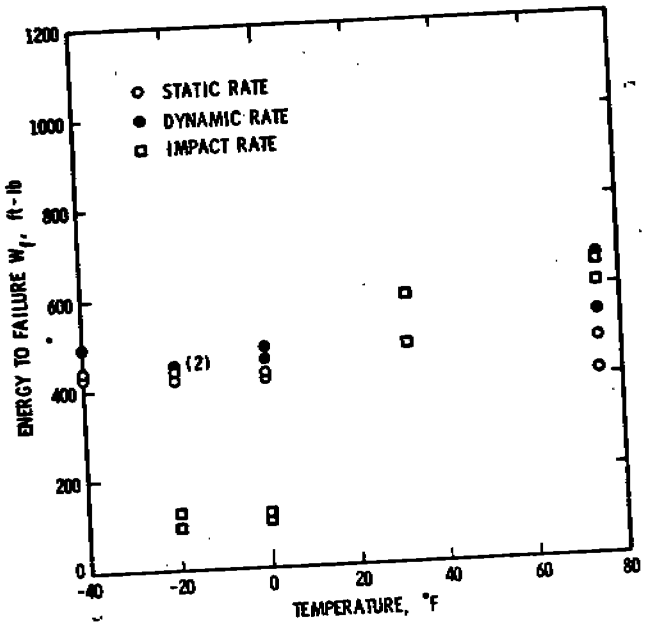

Figure 28. Temperature Dependence of DT Energy-to-Failure W_f, Heat No. 4 (ABS-CS)

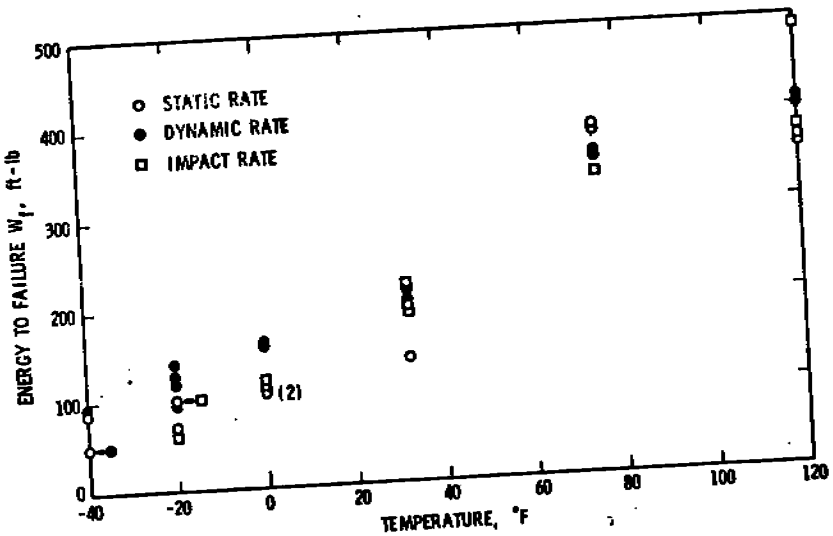

Figure 29. Temperature Dependence of DT Energy-to-Failure W_f, Heat No. 6 (A517-D)

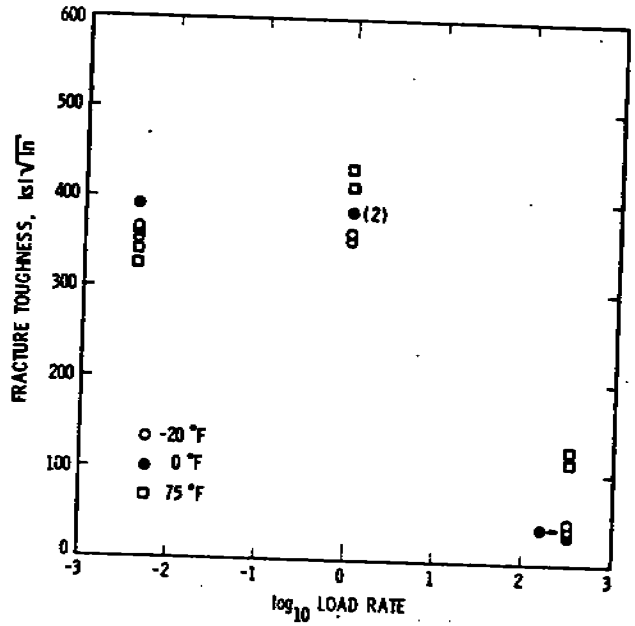

Figure 30. Rate Dependence of DT Fracture Toughness, Heat No. 4 (ABS-CS)

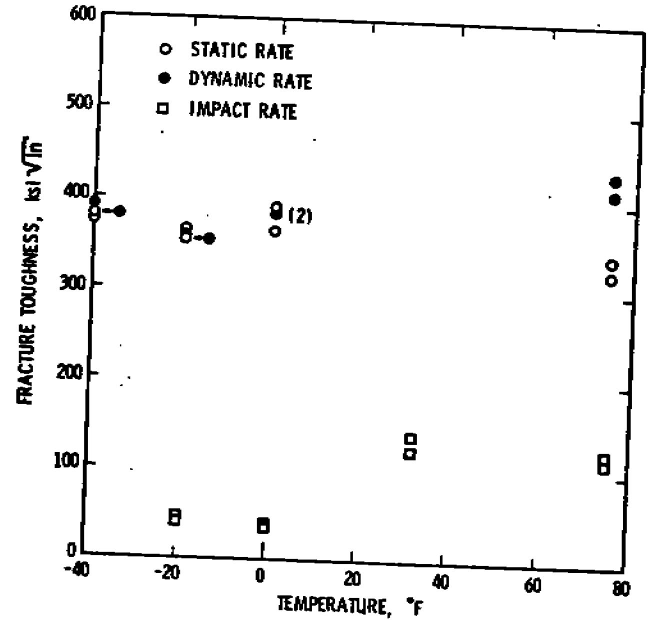

Figure 31. Temperature Dependence of Fracture Toughness, Heat No. 4 (ABS-CS)

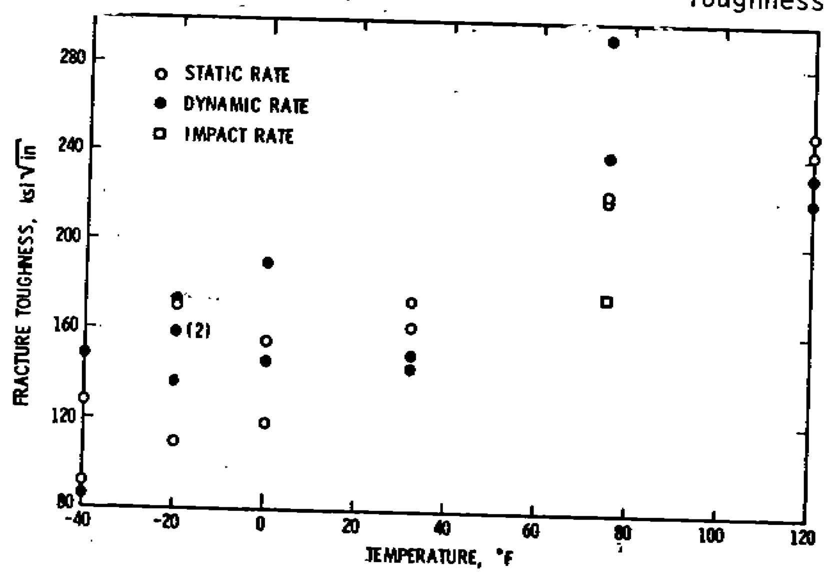

Figure 32. Temperature Dependence of Fracture Toughness, Heat No. 6 (A517-D)

large when viewed on a toughness basis. That is, at the slow rate, the material is on the upper shelf at -40°F while at impact conditions, the material is on the lower shelf at +80°F. If one assumes that crack initiation coincides with the maximum load, then the dynamic toughness as measured in this program indicates that a fatigue crack can extend very easily under a rapid load situation, even when the temperature is considerably above the conventionally determined transition. Since the total energy to failure is sizable, this does mean that crack propagation takes place in a ductile fashion, thereby indicating that considerable energy is dissipated by the propagation process.

There are similar data for the A517 at 75°F. Here, the energy to failure is about the same for all three rates of loading. The total energies are even lower for the A517 than the CS material; however, the dynamic toughness of the A517 is almost 50 percent greater. This suggests that the A517 is more resistant to crack initiation, but it is less resistant to crack propagation as the total energy absorbed is fairly small. Again, one must be cautious about such a conclusion on the basis of a single experiment, particularly as Heat 5, A517, shows a much higher energy to failure than does Heat 6.

Some scatter must be expected in yield point P_Y data, especially at higher temperatures and/or lower load rates where ductility is more prominent. Under these conditions it is difficult to identify yield point load consistently for all records. However, the data indicate how yield load for the DT specimen increases with load rate at room temperatures for CS plate where ductility precludes brittle failure. At temperatures below the transition temperature the yield point load P_Y decreases with the load rate; in these cases where failure is governed by brittle cleavage, the yield load is coincident with maximum load. The yield load increases through the transition temperature region, especially at higher load rates.

As brought out earlier, energy-to-failure W_f drops off with load rate, except at higher temperatures where ductility precludes low energy brittle behavior. Likewise, fracture toughness generally decreases with load rate, and increases with temperature.

V. DISCUSSION OF RESULTS

A. Relation to SSC-244 Criterion

In their report on fracture control guidelines for welded steel ship hulls,[1] Rolfe, et. al., set out a tentative criterion for qualifying toughness and crack arrest properties of ship plate. One of the principal objectives of the present SR-231 program has been to evaluate the proposed Rolfe criterion in light of data generated on parent materials and weldments. Therefore, it is necessary to summarize the SSC-244 criterion before beginning a discussion of the significance of the present data.

The principal factors considered to be of importance in developing the SSC-244 criterion for controlling the susceptibility of welded ship structure to brittle fracture were:

1. Material toughness at the particular service temperature, loading rate, and plate thickness.

2. Size of flaw at the point of fracture initiation, regardless of whether the flaw is an arc strike or a large fatigue crack.

3. Stress level, including residual stress.

The purpose was to develop a criterion for the assurance of adequate fracture resistance of ship steels and weldments in service environments.

The criterion proposed in Ref. 1 can be summarized in the following three propositions:

1. Parent material, weld regions and HAZ regions in primary structure must have an NDT (as measured by the DW-NDT test) no higher than 0°F. Parent materials, weld and HAZ regions used in secondary structure must have an NDT no higher than +20°F.

2. To insure that toughness is satisfactory, 5/8-inch DT tests at 75°F on parent, weld, and HAZ specimens must result in absorbed energy levels no less than E_{75}:

$$E_{75} = \frac{25}{6} (\sigma_y + 20)$$

where

σ_y is the static yield strength in ksi and E_{75} is in ft-lbs.

3. Fail safe design can be achieved through the use of crack arrestor strips. Parent materials used for crack arrestors must meet or exceed the following absorbed energy level E_{32} as measured on 5/8-inch DT specimens tested at 32°F:

$$E_{32} = \frac{10}{3} (\sigma_y + 140)$$

where

σ_y is the static yield strength in ksi and E_{32} is in ft-lb.

The first of these propositions, relating to the DW-NDT test, does not concern the present investigation, although it is treated in some detail in the companion report, SSC-276[3]. The second and third propositions, however, are closely connected with the work reported herein. SSC-244 makes a case that the toughness of ship hull steels should be analyzed using K_{Cd}/σ_{yd} values, i.e., the ratio of the dynamic fracture toughness to the dynamic yield strength. This should become accepted practice, it is argued, because ships can be subjected to dynamic loadings and that K_{Cd}/σ_{yd} values to establish required toughness levels will result in conservative design at lower loading rates. Therefore, in order to evaluate the validity of the SSC-244 criterion against the present data, it is necessary to examine K_C/σ_y and how this ratio varies with load rate.

SSC-244 introduced the assumption that at 75°F, $\sigma_{yd} = \sigma_y +$ 20 ksi where σ_y is the "static" yield strength. Analysis of the present data, as summarized in Table 7, suggests that adding 20 ksi to the static yield strength to obtain σ_{yd} will lead to high estimates for σ_{yd} in the high strength Q&T steels. These materials are less rate-sensitive than are the as-rolled and normalized steels. However, the 20 ksi "impact yield overstress" assumption will result in low estimates for σ_{yd} for normalized steels characterized as having predominately Bainite microstructures.

SSC-244 introduced the minimum toughness requirement that $K_{Cd} = 0.9\ \sigma_y$ at 32°F and $K_{Cd} = 1.5\ \sigma_y$ at 75°F. These relationships are beyond the usual plane strain fracture toughness parameters and indicate that crack tip plasticity is assumed to exist in order to achieve these high (dynamic) toughness values. It is difficult to make a direct comparison of the present data base with the above requirements, primarily because the present data all were obtained from precracked DT specimens, while the SSC-244 refers to press-notched DT specimens. Work performed on SR-224[3] indicated that the energy-to-failure for the press-notched specimen was higher than for the precracked specimen, at all temperatures. However, these conclusions refer to total energy-to-failure, W_f, and not to the energy to maximum load W_m, which is related directly to K_{Cd}.

Although the particular test matrix in the program is somewhat limited, toughness comparisons for the CS and A517 material can be made. Referring to the data at 75°F for the impact conditions

	σ_{yd}	K_{Cd}	K_{Cd}/σ_{yd}	W_F	E_{75}
CS	73.0	121	1.66	625	283
A517	133.6	176	1.32	335	617

From these data, one sees that the CS material meets the minimum K_{Cd}/σ_{yd} value of 1.5, while the A517 does not. Moreover, the A517 does not meet the dynamic tear energy requirement by a large measure whereas the CS plate does. It will be recalled that these data were interpreted to indicate that the CS material is less resistant to crack initiation, but once initiated, the crack would appear to dissipate energy in a ductile mode. On the other hand, the higher K_{Cd} of the A517 indicates more resistance to crack initiation but the lower DT energy means that there is less plastic deformation during actual propagation. In spite of this, the higher value of K_{Cd}/σ_{yd} indicates that in structural applications, the thickness of the plate may play a role by allowing the development of non-plane strain behavior, hence reducing the tendency for catastrophic failure in the CS plate.

It should also be noted that these results are obtained for precracked specimens. This points up the necessity for being aware of the different components of the proposed criterion. That is, while high levels of energy dissipation during rapid crack propagation are desirable, the fundamental requirement should be that the material shows high resistance to the initiation of fast fracture in the first place. This suggests that the use of the total energy to failure may not be enough and that some method of "initiation" energy such as the W_m used in this program may be necessary. For example, if the CS plate in the present study were slightly less tough, i.e. < 110 ksi $\sqrt{\text{in.}}$, it could display excellent W_f values but still be undesirable from an "initiation" toughness view.

This is, of course, consistent with the earlier remarks of the notch effects. There it was argued that the lower strength materials developed full thickness plasticity during crack initiation. Hence, the pressed notch showed more energy absorption. Conversely, the higher strength alloys began to cleave before the through thickness constraint effect was lost.

It is also important to note that the toughness values obtained from the DT impact test are not always strongly conservative. Of the materials tested, EH-32, CS, A678, and A537 showed sizable shifts in the DT energy-temperature curve with increasing rate; the DS, AH-32, B, and A517 did not. For example, at 75°F, three K_C/σ_Y ratios, were found:

	Impact	Dynamic	Quasi-Static
CS	1.66	7.20	6.96
A517	1.32	2.12	1.73

Thus, the relative toughness values also show a large rate effect for the CS but not for the A517. While comparable data for the other materials are not available, large variations in the different materials were found during the course of this project. For the intermediate rate (dynamic) toughness divided by the yield stress is about 1.6 at 0°F for the AH-32 material. This value is much lower than the comparable 5.2 for the EH-32 at 0°F.

While all the data generated under the present program indicate that K_C/σ_Y increases as the load rate is reduced from impact values, the amount of the increase depends on the particular material. This supports the SCC-244 assertion that designing to impact rates is conservative, although it is not necessarily strongly conservative as implied in that document.

As specifically applied to actual ship loading rates, it was suggested in Section I-B that the maximum strain rate observed during slamming is about 1×10^{-1} in/in/sec. This rate is, therefore, slightly less than the rate used in the dynamic tests in this project. Based on the data for the two materials, CS and A517, it is clear that there would not be much advantage to basing design data on a dynamic test since the relative toughness is not much different than the statically obtained values. On the other hand,there is a significant difference between the dynamic and impact values for the CS, while there is less of a difference for the A517. This then merely indicates that if it is desirable to account specifically for rate effects, then the materials will have to be tested at those desired rates. Faster rates can be applied, but because of the differences in material behavior, there is no way to determine the extent of the conservatism a priori.

Moreover, if an impact test is to be used, it makes sense to use a precracked DT specimen to account for the response of the material to the sharp fatigue crack rather than the more blunt press notch. While this additional effort makes the test less convenient, it does increase its value by providing a means to examine the real problems, i.e., the load suddenly applied to a member with a sharp crack. The differentiation between the energy of initiation and propagation is also valuable. The methods of accomplishing this are somewhat imprecise but they should help in identifying a material which has low toughness but readily forms shear lips and dissipates considerable energy during propagation.

B. Assessment

The experimental results generally validate the assumptions made in developing the proposed SSC-244 criterion. Two overall observations are pertinent to an assessment of the present results. First, there were too few data points distributed across a test matrix containing an enormously large number of possible combinations of heat, rate, temperature, and derived data, not to mention scatter inherent in these types of tests. This paucity of data made it possible to examine trends in the rate and temperature dependence of σ_Y and K_C, but limited detailed interpretation. Second, it was clear that one may expect to find substantial heat-to-heat variations in the yield and toughness properties of ship steel. That is, a rational fracture toughness criterion for ship structures should account for statistical variations in mechanical properties within a given heat, and also across a population of nominally identical heats.

The limitations mentioned above made it difficult to characterize dynamic yield strength σ_{yd} reliably for some heats. This strength parameter depends upon the activation volume of the process, which in turn depends upon $\partial \sigma_Y / \partial \ln \dot{\varepsilon}$, or the rate-of-change of yield strength with strain rate. These measurements are difficult to make consistently, and therefore it was decided to group the findings by type of steel. Due, however, to the difficulty of the tests and to the paucity of data, these conclusions must be regarded as tentative from a quantitative viewpoint.

The calculations leading to Eq. (10) indicate that there is a temperature, common to all material heats, at which σ_{yd} is the same as the static yield strength at room temperature. This is an interesting concept, worthy of additional experimental investigation to determine its validity and accuracy.

Relative to the proposed fracture criterion, the data obtained in this program suggest that:

1. In terms of load carrying capability, the high strength materials provide more load carrying capacity before failure. On the other hand, once fast fracture begins, it will be difficult to stop without sizable crack arrestors. Conversely, the low strength materials can carry less load to failure but because of their ductile fast fracture mode, will be easier to arrest.

2. The foregoing implies that a design philosophy must be clearly fixed. The high strength materials offer potential for maximum performance at higher risk unless a redundant structure - crack arrest method is employed. For the lower strength alloys, the lower performance is balanced by the higher resistance to fast fracture.

3. In the event that additional data supports these points, it may well be necessary to develop separate design criteria for high and low strength materials, to avoid excessive conservatism in the case of low strength materials if the fracture resistance is based on high strength materials. If the approach is based on low strength materials only, then the high strength materials will be excluded from use or may have inadequate fracture resistance.

Project SR-224 and SR-231 may be regarded as the first steps in validating a fracture toughness and fracture control criterion for ship structure. The present investigation supported the credibility of the SSC-244 proposed criterion in general terms. It also showed, as would be expected, that the detailed temperature and rate dependence of K_{Cd}/σ_{yd} depends upon the material and heat in question. It seems reasonable, therefore, that future efforts along these lines should be directed at filling in the gaps in the present data bank, and at evaluating the statistics of specimen-to-specimen and of heat-to-heat variations in properties.

VI. RECOMMENDATIONS

1. The primary need disclosed by this project is the additional data needed on selected high and low strength materials. The partitioning of data, as done in the report, into high and low strength behavior is based, however reasonably, on incomplete data. A much more intensive test program on a few materials is needed. This program should include:

    a. Multiple DT curves as a function of temperature.

    b. Characterization of press notch vs fatigue notch.

    c. Energy to failure and energy to maximum load.

    d. Metallographic analysis of the fracture surfaces.

    e. Selected dynamic (non-impact) comparisons.

    These tests should be performed on two, or at most three, rather than the eight materials in this program.

2. An analysis of data resulting from the preceding would then determine whether the proposed criterion should be split into separate categories or modified in some other fashion.

3. Further analytical and experimental investigation of the dynamic, elasto-plastic response of the 5/8-inch press-notch DT specimen needs to be undertaken, so that sensible limits can be imposed on its use as a qualification test in the proposed criterion. This effort is also needed to tie the DT test to dynamic fracture toughness.

4. To supplement and clarify the rate requirements, better definition of actual shipboard loading rates is needed. Some of this is available in Ship Structure Reports but it is not directed at rate effects and hence is not in a readily usable form. These data should be examined carefully.

5. Additional experimental effort is needed to establish the validity of Equation (10), which determines how much the static room temperature yield strength is changed by load rate and temperature. It should be established whether the activation Volume V can be partitioned into representative values for classes of ship steels as was done tentatively in this report. Also, whether there is a temperature near 328°F at which the impact yield strength matches that at room temperature, static conditions for all heats should be explored in more detail. If this result is in fact valid, it would simplify the determination of σ_{yd} by allowing these tests to be conducted under equivalent static, room temperature conditions.

6. These recommendations need to be merged with those from Report SSC-276 (on welded structure) for further evaluation of the proposed SSC-244 criterion.

REFERENCES

1. Rolfe, S. T., Rhea, D. M. and Kuzmanovic, B. O., "Fracture-Control Guidelines for Welded Steel Ship Hulls," Ship Structure Committee Report SSC-244, 1974.

2. Hawthorne, J. R. and Loss, F. J., "Fracture Toughness Characterization of Shipbuilding Steels," Ship Structure Committee Report SSC-248, 1975.

3. Francis, P. H., Cook, T. S. and Nagy, A., "Fracture Behavior Characterization of Ship Steels and Weldments," Ship Structure Committee Report SSC-276. 1978.

4. Krafft, J. M., and Sullivan, A. M., "Effects of Speed and Temperature on Crack Toughness and Yield Strength," ASM Transactions, Vol. 56, 1963, pp. 160-175.

5. Eftis, J. and Krafft, J. M., "A Comparison of the Initiation With Rapid Propagation of a Crack in a Mild Steel Plate," J. of Basic Engineering, Trans. ASME, Series D, 87, 1965, p. 257-263.

6. Shoemaker, A. K., "Factors Influencing the Plane-Stress Crack Toughness Values of a Structural Steel," J. of Basic Engineering, Trans. ASME, Series D, 91, p. 506-511.

7. Shoemaker, A. K., and Rolfe, S. T., "Static and Dynamics How Temperature K_{IC} Behavior of Steels," J. of Basic Engineering, Trans. ASME, Series D, 91, 1969, p. 512-518.

8. Shoemaker, A. K. and Rolfe, S. T., "Static and Dynamic Low Temperature Crack Toughness Performance of Seven Structural Steels," Engineering Fracture Mechanics, 2, 1971, p. 319-339.

9. Lewis, E. V., and Zubaly, R. B., "Dyanmic Loadings Due to Waves and Ship Motions," Paper M, SNAME Ship Structure Symposium of October 6-8, 1975, Washington, D.C.

10. Henry, J. R., and Bailey, F. C., "Slamming of Ships: A Critical Review of the Current State of Knowledge," Ship Structure Committee Report SSC-208, 1970.

11. "Proposed Method for 5/8-in. (16-mm) Dynamic Tear Test of Metallic Materials," 1976 Annual Book of ASTM Standards, Part 10, 777-784.

12. Cottrell, A. H. and Aytekin, V., Journal of the Institute of Metals, Vol. 77, 389 (1950).

13. Davidson, D. L., and Lindholm, U. S., "The Effect of Barrier Shape in the Rate Theory of Metal Plasticity," Proceedings of Conference on Mechanical Properties of Materials at High Strain Rates, Institute of Physics, Conference Series 21, Bristol, England, 1974, pp. 124-137.

14. "Toughness Evaluation of Electrogas and Electroslag Weldments," Bethlehem Steel Corp., Final Report on MARAD-ABS Program, March, 1975.

UNCLASSIFIED

SECURITY CLASSIFICATION OF THIS PAGE (When Data Entered)

REPORT DOCUMENTATION PAGE

READ INSTRUCTIONS BEFORE COMPLETING FORM

1. REPORT NUMBER: SSC-275
2. GOVT ACCESSION NO.
3. RECIPIENT'S CATALOG NUMBER
4. TITLE (and Subtitle): THE EFFECT OF STRAIN RATE ON THE TOUGHNESS OF SHIP STEELS
5. TYPE OF REPORT & PERIOD COVERED: Final Technical Report
6. PERFORMING ORG. REPORT NUMBER
7. AUTHOR(s): P. H. Francis, T. S. Cook and A. Nagy
8. CONTRACT OR GRANT NUMBER(s): N00024-75-C-4284
9. PERFORMING ORGANIZATION NAME AND ADDRESS: Southwest Research Institute, San Antonio, TX 78284
10. PROGRAM ELEMENT, PROJECT, TASK AREA & WORK UNIT NUMBERS
11. CONTROLLING OFFICE NAME AND ADDRESS: Dept. of the Navy, Naval Sea Systems Command, Washington, D.C. 20362
12. REPORT DATE: April, 1978
13. NUMBER OF PAGES: 64
14. MONITORING AGENCY NAME & ADDRESS (if different from Controlling Office): Ship Structure Committee, U.S. Coast Guard Headquarters, Washington, D.C. 20590
15. SECURITY CLASS. (of this report): UNCLASSIFIED

15a. DECLASSIFICATION/DOWNGRADING SCHEDULE

16. DISTRIBUTION STATEMENT (of this Report): UNLIMITED
17. DISTRIBUTION STATEMENT (of the abstract entered in Block 20, if different from Report): UNLIMITED
18. SUPPLEMENTARY NOTES
19. KEY WORDS (Continue on reverse side if necessary and identify by block number)
20. ABSTRACT (Continue on reverse side if necessary and identify by block number)

Yield strength and fracture toughness, as measured by the dynamic tear test, were determined as a function of load rate and temperature for several ship primary structure steels in strength ranges up to 100 ksi. The materials used were ABS-B, DS, AH-32, EH-32, CS, A517-D, A678-C, and A537-B, in one or two heats each. The effect of notch geometry, i.e., fatigue precracked vis-a-vis pressed notch, was investigated in some of the tests.

By fully instrumenting some of the tests, the energy to maximum load as well as the total energy to failure was determined. Based on these energies, the resistance of the materials to crack initiation and to propagation could be examined. The results indicate potentially different fracture behavior between the high and low strength alloys. This in turn has implications in terms of the Ship Structure Committee Report SSC-244 proposed fracture criterion for qualifying toughness and crack arrest properties of ship steels and weldments.

METRIC CONVERSION FACTORS

Approximate Conversions to Metric Measures

Symbol	When You Know	Multiply by	To Find	Symbol
		LENGTH		
in	inches	*2.5	centimeters	cm
ft	feet	30	centimeters	cm
yd	yards	0.9	meters	m
mi	miles	1.6	kilometers	km
		AREA		
in^2	square inches	6.5	square centimeters	cm^2
ft^2	square feet	0.09	square meters	m^2
yd^2	square yards	0.8	square meters	m^2
mi^2	square miles	2.6	square kilometers	km^2
	acres	0.4	hectares	ha
		MASS (weight)		
oz	ounces	28	grams	g
lb	pounds	0.45	kilograms	kg
	short tons (2000 lb)	0.9	tonnes	t
		VOLUME		
tsp	teaspoons	5	milliliters	ml
Tbsp	tablespoons	15	milliliters	ml
fl oz	fluid ounces	30	milliliters	ml
c	cups	0.24	liters	l
pt	pints	0.47	liters	l
qt	quarts	0.95	liters	l
gal	gallons	3.8	liters	l
ft^3	cubic feet	0.03	cubic meters	m^3
yd^3	cubic yards	0.76	cubic meters	m^3
		TEMPERATURE (exact)		
°F	Fahrenheit temperature	5/9 (after subtracting 32)	Celsius temperature	°C

*1 in = 2.54 (exactly). For other exact conversions and more detailed tables, see NBS Misc. Publ. 286, Units of Weights and Measures, Price $2.25, SD Catalog No. C13.10:286.

☆ U.S. GOVERNMENT PRINTING OFFICE: 1978—725-241/509

Approximate Conversions from Metric Measures

Symbol	When You Know	Multiply by	To Find	S
		LENGTH		
mm	millimeters	0.04	inches	
cm	centimeters	0.4	inches	
m	meters	3.3	feet	
m	meters	1.1	yards	
km	kilometers	0.6	miles	
		AREA		
cm^2	square centimeters	0.16	square inches	
m^2	square meters	1.2	square yards	
km^2	square kilometers	0.4	square miles	
ha	hectares (10,000 m^2)	2.5	acres	
		MASS (weight)		
g	grams	0.035	ounces	
kg	kilograms	2.2	pounds	
t	tonnes (1000 kg)	1.1	short tons	
		VOLUME		
ml	milliliters	0.03	fluid ounces	
l	liters	2.1	pints	
l	liters	1.06	quarts	
l	liters	0.26	gallons	
m^3	cubic meters	35	cubic feet	
m^3	cubic meters	1.3	cubic yards	
		TEMPERATURE (exact)		
°C	Celsius temperature	9/5 (then add 32)	Fahrenheit temperature	

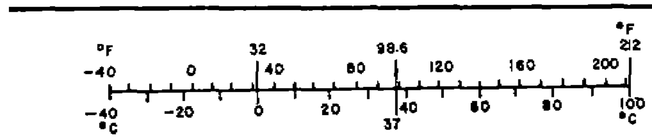

SHIP RESEARCH COMMITTEE
Maritime Transportation Research Board
National Academy of Sciences-National Research Council

The Ship Research Committee has technical cognizance of the interagency Ship Structure Committee's research program:

MR. O. H. OAKLEY, Chairman, *Consultant, McLean, Virginia*
MR. M. D. BURKHART, *Head, Marine Science Affairs, Office of Oceanographer of the Navy*
DR. J. N. CORDEA, *Senior Staff Metallurgist, ARMCO Steel Corporation*
MR. D. P. COURTSAL, *Vice President, DRAVO Corporation*
MR. E. S. DILLON, *Consultant, Silver Spring, Maryland*
DEAN D. C. DRUCKER, *College of Engineering, University of Illinois*
MR. W. J. LANE, *Consultant, Baltimore, Maryland*
DR. W. R. PORTER, *Vice Pres. for Academic Affairs, State University of New York Maritime College*
MR. R. W. RUMKE, *Executive Secretary, Ship Research Committee*

The Ship Materials, Fabrication, and Inspection Advisory Group prepared the project prospectus and evaluated the proposals for this project:

DR. J. N. CORDEA, Chairman, *Senior Staff Metallurgist, ARMCO Steel Corporation*
MR. J. L. HOWARD, *President, Kvaerner-Moss, Inc., N.Y.*
MR. J. G. KAUFMAN, *Manager, Technical Development, Aluminum Company of America*
MR. T. E. KOSTER, *Naval Architect, AMOCO International Oil Company*
DR. H. I. McHENRY, *National Bureau of Standards, Boulder, CO*
PROF. P. F. PACKMAN, *Materials Science & Metallurgical Engrg. Dept. Vanderbilt University*
PROF. S. T. ROLFE, *Civil Engineering Dept., University of Kansas*
PROF. G. C. SIH, *Inst. of Fracture & Solid Mechanics, Lehigh University*

The SR-1231 *ad hoc* Project Advisory Committee provided the liaison technical guidance, and reviewed the project reports with the investigator:

DR. J. N. CORDEA, Chairman, *Senior Staff Metallurgist, ARMCO Steel Corporation*
DR. H. I. McHENRY, *National Bureau of Standards, Boulder, CO*
PROF. S. T. ROLFE, *Civil Engineering Dept., University of Kansas*
PROF. G. C. SIH, *Inst. of Fracture & Solid Mechanics, Lehigh University*

SHIP STRUCTURE COMMITTEE PUBLICATIONS

These documents are distributed by the National Technical Information Service, Springfield, Va. 22151. These documents have been announced in the Clearinghouse journal U.S. Government Research & Development Reports (USGRDR) under the indicated AD numbers.

SSC-260, *A Survey of Fastening Techniques for Shipbuilding* by N. Yutani and T. L. Reynolds. 1976. AD-A031501.

SSC-261, *Preventing Delayed Cracks in Ship Welds - Part I* by H. W. Mishler. 1976. AD-A031515.

SSC-262, *Preventing Delayed Cracks in Ship Welds - Part II* by H. W. Mishler. 1976. AD-A031526.

SSC-263, (SL-7-7) - *Static Structural Calibration of Ship Response Instrumentation System Aboard the Sea-Land McLean* by R. R. Boentgen and J. W. Wheaton. 1976. AD-A031527.

SSC-264, (SL-7-8) - *First Season Results from Ship Response Instrumentation Aboard the SL-7 Class Containership S.S. Sea-Land McLean in North Atlantic Service* by R. R. Boentgen, R. A. Fain and J. W. Wheaton. 1976. AD-A039752.

SSC-265, *A Study of Ship Hull Crack Arrester Systems* by M. Kanninen, E. Mills, G. Hahn, C. Marschall, D. Broek, A. Coyle, K. Masubushi and K. Itoga. 1976. AD-A040942

SSC-266, *Review of Ship Structural Details* by R. Glasfeld, D. Jordan, M. Kerr, Jr., and D. Zoller. 1977. AD-A040941.

SSC-267, *Compressive Strength of Ship Hull Girders - Part III - Theory and Additional Experiments* by H. Becker and A. Colao. 1977. AD-A047115.

SSC-268, *Environmental Wave Data for Determining Hull Structural Loadings* by D. Hoffman and D. A. Walden. 1977. AD-A047116.

SSC-269, *Structural Tests of SL-7 Ship Model* by W. C. Webster and H. G. Payer. 1977. AD-A047117.

SSC-270, *Gross Panel Strength Under Combined Loading* by A. E. Mansour. 1977. AD-A049337.

SSC-271, *A Correlation Study of SL-7 Containership Loads and Motions - Model Tests and Computer Simulation* by P. Kaplan, T. P. Sargent, and M. Silbert. 1977. AD-A049349.

SSC-272, *In-Service Performance of Structural Details* by C. R. Jordan and C. S. Cochran. 1978.

SSC-273, *Survey of Structural Tolerances in the U.S. Commercial Ship-Building Industry* by N. S. Basar and R. F. Stanley. 1978.

SSC-274, *Development of an Instrumentation Package to Record Full-Scale Ship Slam Data* by E. G. U. Band and A. J. Euler. 1978.